Uniform, Independent Bifunctionalization of a Metal-Organic Framework Material

by

Christopher S. Satterfield

B.S., Northwestern Oklahoma State University, 2015

A THESIS

submitted in partial fulfillment of the requirements for the degree

MASTER OF SCIENCE

Department of Chemistry
College of Arts and Sciences

KANSAS STATE UNIVERSITY
Manhattan, Kansas

2018

Abstract

Molecular architecture involves the assembly of molecular building blocks to form supramolecular structures and the decoration of their interiors. The evolution and gathering of molecular building blocks into supramolecular constructs include examples such as co-crystals, micelles, nanoparticles, etc. These cases offer novel and advantageous pathways for research in supramolecular chemistry, however, a class of materials known as metal-organic frameworks (MOFs) materials has emerged as a prime candidate for molecular construction and interior design.

MOFs are highly tunable materials because they can be synthesized from a wide range of metals cations and organic linkers. The organic linkers can also be functionalized after the MOF material has been synthesized through a process known as post-synthetic modification (PSM). These materials can be synthesized using two different organic linkers, resulting in a mixed-ligand MOF. If these ligands are modifiable and react independently, the resulting MOF structure will be orthogonally functionalized. Upon PSM we hypothesize that our porous, mixed-ligand MOF will contain homogenous bifunctionality as a blueprint for the construction of a uniformly orthogonally functionalized MOF. The synthesis of the first metal-organic framework, KSU-1, is the first of its kind to be developed at Kansas State University. PSM strategies used in this research show successful functionalization of each organic linker leading to uniform bifunctionality throughout our material. Characterization studies commonly used with MOFs verifies the synthesis and PSM of KSU-1.

Table of Contents

List of Figures

List of Schemes

Chapter 1: Introduction

Molecular Architecture

Molecular architecture involves the assembly of molecular building blocks to form supramolecular structures, and the decoration of their interiors.[1] The evolution and gathering of molecular building blocks into supramolecular constructs include examples such as co-crystals,[2] micelles,[3] nanoparticles,[4] etc. These cases offer novel and advantageous pathways for research in supramolecular chemistry, however, a class of materials known as metal-organic frameworks (MOFs) materials has emerged as a prime candidate for molecular construction and interior design.

Introduction to Metal-Organic Frameworks Materials

Metal-organic frameworks materials are a class of porous solids that have emerged as a front runner in supramolecular chemistry over the last two decades.[5,36] MOF materials are crystalline, three-dimensional porous materials that are synthesized by the self-assembly of metal cations with organic molecules. The resulting materials assemble as highly ordered frameworks, or grids, with the metal cluster at the corners and are connected by organic linkers (Scheme 1).[5]

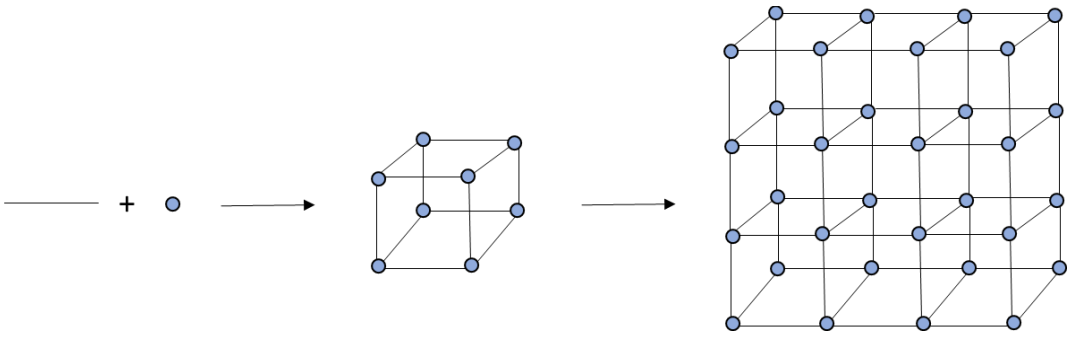

Scheme 1. Schematic representation for a metal-organic framework where the black line represents an organic ligand and the blue circle represents a metal cation.

MOFs are highly tunable materials that are synthesized from a wide range of metal cations and organic linkers, providing a constant evolution of their architectural and chemical properties, as well as their applications in catalysis,[6] gas storage,[7] sensing,[8] gas separations,[9] drug delivery,[10] etc. These microporous materials transcend other microporous rivals due to the availability of a variety organic of linkers resulting in an array of pore topologies and chemical environments allowing MOFs to be a highly competitive field in chemistry research today.

Design of Metal-Organic Frameworks

The growth and development of MOFs have advanced thanks in large part to novel methods of design and synthesis leading to highly complex porous materials. Organic ligands for MOFs are often pre-synthesized for chosen functionality. The tunability of MOFs stem from the functionalizablility of these organic ligands pre- and post MOF assembly.[11] Yaghi *et al.* pioneered the first synthesis of MOFs in 1999 using solvothermal synthesis leading to the novel creation of some of the first well-known MOFs that are still widely used today.[14] When MOFs came into prevalence this method of synthesis offered a simple, yet difficult process of making these porous structures. [12-13]

Synthesis of Metal-Organic Frameworks: Solvothermal Synthesis

Solvothermal synthesis (Scheme 2), the traditional route of building MOFs, involves placing organic linkers and a metal salt in a solvent and heating the reaction mixture to a desired temperature.[15] This process requires specific reaction conditions for the MOF crystals to nucleate. Conditions such as temperature, ligand and metal concentration,

solvent type, time, and even the vessel used for growth are all variables necessary for MOFs to form.[15,37] This process, although easy to set-up, limits the process of synthesizing MOFs because of their specific growing conditions. Indeed, because of growth specificity the process of developing a MOF system that is fashioned for desired applications is labor-intensive, limiting MOF chemistry.[17] To address this issue, MOF chemists developed methodologies to tap into unattainable frameworks, a practice that we would like to take advantage of and develop our own synthetic tool. One such methodology that we take full advantage of to prompt our synthetic endeavors is postsynthetic modification (PSM).[11]

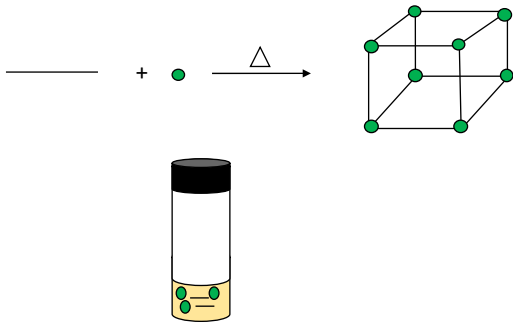

Scheme 2. A representation of solvothermal synthesis in a vial, a typical growing environment for MOFs. The black line represents the organic ligand and the green circle represents the metal node.

Postsynthetic Modification, Multifunctional, and Multivariate MOFs

PSM (Scheme 3) is a useful synthetic strategy that can only be undertaken upon completion of solvothermal synthesis. This strategy entails the modification of functional groups using liquid-solid state reactions on the MOF ligands to form new functionalities.[11] The term "postsynthetic modification" was coined by Seth Cohen *et al.* in 2007 during his demonstration of modifying IRMOF-3, a MOF composed of -NH_2 bearing linkers. The

amines were reacted with acetic anhydride resulting in an amide-functionalized MOF material.[17]

This strategy is advantageous due to the potential to reach newly designed MOFs that are inaccessible through solvothermal synthesis. PSM is also a gateway to produce MOFs that have several functions through different chemical properties. A MOF can be modified with one or multiple functions leading to multifunctional multivariate MOFs (MTV MOFs).

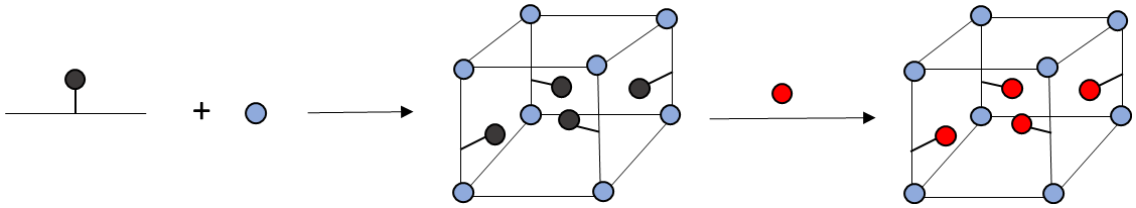

Scheme 3. A representation of PSM where a reaction takes place on a functional group that the MOF has after solvothermal synthesis and is reacted on to form a new functionality.

Multifunctional MOFs are frameworks that provide multiple functions.[18-19] Since multifunctional MOFs ascended into the fold of porous coordination polymers, researchers have accessed new levels of complexity and diversity.[18] Multivariate MOFs are frameworks that are multifunctional, but lack uniformity because each pore of the MOF can be different from the next.[20] Multivariate MOFs attain their characteristics via ligand modification, metalation, surface functionalization, and so forth.[21]

We would like to tackle the problem of variance for multifunctional MOFs by forming a uniformly multifunctionalized MOF. Using PSM we can have a material that not only has multiple functions but has high selectivity and predictability for application-based usage. One such framework that acts as a blueprint for multifunctionality is a mixed-ligand framework. A mixed ligand framework has different ligands connected to the metal corners

in a well-defined manner.[21] A tool that we can take advantage of, together with mixed-ligand MOFs, to provide our uniform multifunctionality is orthogonal functionalizability.

Orthogonal Functionalization

Orthogonality, in chemistry is when two or more functionalities on the same substance react independently from one another with different reactants. [22-28] Orthogonal chemistry is widely used in supramolecular constructs,[22-24] organic synthesis,[25] and in biological settings.[26-28] Orthogonal functionality has already been established for MOFs by Rosi *et al.* Their methods were to independently functionalize linkers that were orthorthogonally functionalizable in their MOF. However, the orthogonally modifiable linkers were unevenly distributed throughout their MOF materials. Had these orthogonal functional groups been distributed homogeneously throughout the MOF they would have achieved a uniform orthogonally functionalized MOF. The problem is unpredictability of orthogonal functionality positioning and has yet to be addressed.[29] This is a goal we would like to accomplish to expand the field of MOF synthesis and design.

Objective

The goal of this project (Scheme 4) is to utilize known synthetic strategies to form a porous, mixed-ligand MOF that is independently functionalized as a groundwork for a uniformly orthogonally functionalized MOF.

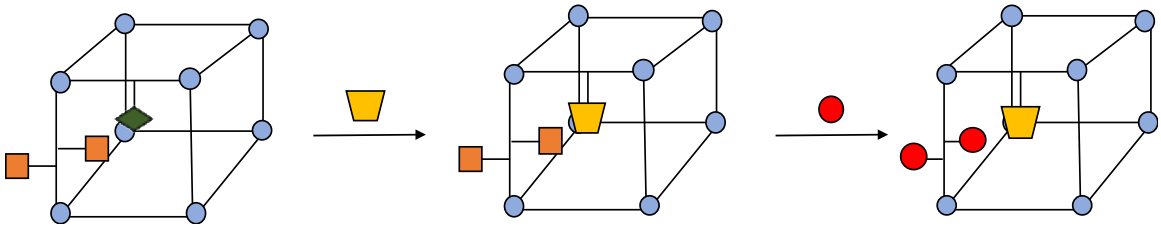

Scheme 4. Schematic diagram of an independently functionalizable MOF as a base for an orthogonally functionalized MOF tool.

Chapter References

1. Heywood, B. R.; Mann, S.; Molecular Construction of Oriented Inorganic Materials: Controlled Nucleation of Calcite and Aragonite under Compressed Langmuir Monolayers. Chemistry Materials 1994, *6*, 311-318.
2. Aakeröy, C. B.; Sinha, A. S.; Co-crystals: Preparation, Characterization and Applications. Royal Chemistry Sociecty 2018, 1-32.
3. Song, W.; Poyraz, A. S.; Meng, Y.; Ren, Y.; Ren, Z.; Chen, S.; Suib, S. L.; Mesoporous Co_3O_4 with Controlled Porosity: Inverse Micelle Synthesis and High-Performance Catalytic CO Oxidation at -60 °C. Chemistry of Materials **2014**, *26*, 4629-4639.
4. Talapin, D. V.; Introduction: Nanoparticle Chemistry. Chemical Reviews **2016**, *116*, 10343-10345.
5. Zhou, H.; Long J. R.; Yaghi, O. M.; Introduction to Metal-Organic Frameworks. Chemical Review **2012**, *112*, 673-674.
6. Chen, Y., Zhang, R.; Jiao, L.; Jiang, H.; Metal-organic framework-derived porous materials for catalysis. Coordination Chemistry Reviews **2018**, *362*, 1-23.
7. Li, B.; Wen, H.; Wang, H.; Wu, H.; Tyagi, M.; Yildirim, T.; Zhou, W.; Chen, B.; A Porous Metal-Organic Framework with Dynamic Pyrimidine Groups Exhibiting Record High Methane Storage Working Capacity. Journal of American Chemical Society **2014**, *136*, 6207-6210.
8. Zhang, M.; Feng, G.; Song, Z.; Zhou, V.; Chao, H.; Yuan, D.; Tan, T. T. Y.; Guo, Z.; Hu, Z.; Tang, B. Z.; Liu, B.; Zhao, D.; Two-Dimensional Metal-Organic Framework with Wide Channels and Responsive Turn-On Fluorescence for the Chemical Sensing of Volatile Organic Compounds. Journal of American Chemical Society **2014**, *136*, 7241-7244.
9. Li, L.; Lin, R.; Krishna, R.; Wang, X.; Li, B.; Wu, H.; Li, J.; Zhou, W.; Chen, B.; Flexible-Robust Metal-Organic Framework for Efficient Removal of Propyne from Propylene. Journal of American Chemical Society **2017**, *139*, 7733-7736.
10. Chen, X.; Tong, R.; Shi, Z.; Yang, B.; Liu, H.; Ding, S.; Wang, X.; Lei, Q.; Wu, J.; Fang, W.; MOF Nanoparticles with Encapsulated Autophagy Inhibitor in Controlled Drug Delivery System for Antitumor. ACS Applied Materials Interfaces **2018**, *10*, 2328-2337.
11. Cohen, S. M.; The Postsynthetic Renaissance in Porous Solids. Journal of American Chemical Society **2017**, *139*, 2855-2863.
12. Das, S.; Kim, H.; Kim, K.; Metathesis in Single Crystal: Complete and Reversible Exchange of Metal Ions Constituting the Frameworks of Metal−Organic Frameworks. Journal of American Chemical Society **2009**, *131*, 3814-3815.
13. Burnett, B. J.; Barron, P. M.; Hu, C.; Choe, W.; Stepwise Synthesis of Metal-Organic Frameworks. Replacement of Structural Organic Linkers. Journal of American Chemical Society **2011**, *122*, 9984-9987.
14. Li, H.; Eddaoudi, M.; O'Keeffe, M.; Yaghi, O. M.; Design and synthesis of an exceptionally stable and highly porous metal-organic framework.

15. Royal Chemistry Society. Solvothermal Synthesis. http://www.rsc.org/publishing/journals/prospect/ontology.asp?id=CMO:0001458&MSID=b802258p (Accessed Sept. 10, 2018).
16. Yuan, S.; Feng, L.; Wang, K.l Pang, J.; Bosch, M.; Lollar, C.; Sun, Y.; Qin, J.; Yang, X.; Zhang, P.; Wang, Q.; Zou, L.; Zhang, Y.; Fang, Y.; Li, J.; Zhou, H.; Stable Metal-Organic Frameworks: Design, Synthesis, and Applications. Advanced Materials **2018**, *30*, 1704303-1704338.
17. Wang, Z.; Cohen, S. M.; Postsynthetic Covalent Modification of a Neutral Metal-Organic Framework. Journal of American Chemical Society **2007**, *129*, 12368-12369.
18. Cao, C.; Shi, Y.; Xu, H.; Zhao, B.; A multifunctional MOF as a recyclable catalyst for the fixation of CO_2 with aziridines or epoxides and as a luminescent probe of Cr(VI). Dalton Transactions **2018**, *47*, 4545-4553.
19.Huang, Y.; Liang, J.; Wang, X.; Cao, R.; Multifunctional metal-organic framework catalysis and tandem reactions. Chemical Society Review **2017**, *46*, 126-157.
20. Silva, P.; Vilela, S. M. F.; Tome, J. P. C.; Almeida Paz, F. A.; Multifuctional Metal-Organic Frameworks: From Academia to Industrial Applications. Chemical Society Review **2015**, *44*, 6774-6803.
21. Deng, H.; Doonan, C. J.; Furukawa, H.; Ferreira, R. B.; Towne, J.; Knobler, C. B.; Wang, B.; Yaghi, O. M.; Multiple Functional Groups of Varying Ratios in Metal-Organic Frameworks. Science **2010**, *327*, 846-850.
22. Chen, D.; Xu, N.; Qui, X.; Cheng, P.; Functionalization of Metal-Organic Framework via Mixed-Ligand Strategy for Selective CO_2 Sorption at Ambient Conditions.
23. Maloch, M.; Thibault, R. J.; Drockenmuller, E.; Messerschmidt, M.; Voit, B.; Russell, T. P. Hawker, C. J. Orthogonal Approaches to the Simultaneous and Cascade Functionalization of Macromolecules Using Click Chemistry. Journal of American Chemical Society **2005**, *127*, 14942-14949.
24. Zhou, Z.; Yan, X.; Cook, T. R.; Saha, M. L.; Stang, P. J.; Engineering Functionalization in Supramolecular Polymer: Hierarchical Self Organization of Truly Orthogonal Non-covalent interactions on a Supramolecular Coordination Complex Platform. Journal of American Chemical Society **2016**, *138*, 806-809.
25. Wei, P.; Yan, X.; Huang, F.; Supramolecular polymers constructed by orthogonal self-assembly based on host-guest and metal-ligand interactions. Chemical Society Reviews, **2015**, *44*, 815-832.
26. Lee, C.; Plunkett, K. N.; Orthogonal Functionalization of Cyclopenta[*hi*]aceanthrylenes. Organic letters **2013**, *15*, 1202-1205.
27. Chrominiski, M.; Lewalska, A.; Karczewski, M.; Gryko, D.; Vitamin B_{12} Derivatives for Orthogonal functionalization. Journal of Organic Chemistry **2014**, *79*, 7532-7542.
28. Ehret, F.; Wu, H.; Alexander, S. C.; Devaraj, N. K.; Electrochemical Control of Rapid Bioorthogonal Tetrazine Litigations for Selective Functionalization of Microelectrodes. Journal of American Chemical Society **2015**, *137*, 8876-8879.
29. Sahloul, K.; Lowary, T. L.; Development of an Orthogonal Protection Strategy for the Synthesis of Mycobacterial Arabinomannan Fragments. Journal of Organic Chemistry **2015**, *80*, 11417-11434.
30. Liu, C.; Luo, T.; Feura, E. S.; Zhang, C.; Rosi, N. L.; Orthogonal Ternary Functionalization of a Mesoporous Metal-Organic Framework via Sequential Postsynthetic Ligand Exchange.

31. Stock, N.; Biswas, S.; Synthesis of Metal-Organic Frameworks (MOFs): Routes to Various MOF Topologies, Morphologies, and Composites. Chemical Reviews **2012**, *112*, 933-969.
32. Howarth, A. J.; Peters, A. W.; Vermeulen, N. A.; Wang, T. C.; Hupp, J. T.; Farha, O. K.; Best Practices for the Synthesis, Activation, and Characterization of Metal-Organic Frameworks. Chemistry of Materials **2017**, *29*, 26-39.
33. Wang, Z.; Cohen, S. M.; Postsynthetic modification of metal-organic frameworks. Chemical Society Review **2009**, *38*, 1315-1329.
34. Lee, Y.; Kim, J.; Ahn, W.; Synthesis of metal-organic frameworks: A mini review. Korean Journal of Chemical Engineering **2013**, *30*, 1667-1680.
35. Chaemchuen, S.; Kabir, N. A.; Zhou, K.; Verpoort, F.; Metal-organic frameworks for upgrading biogas *via* CO_2 adsorption to biogas green energy. Chemical Society Review **2013**, *42*, 9304. Journal of American Chemical Society **2015**, *137*, 10508-10511.
36. Lee, J.; Kwak, J. H.; Choe, W.; Evolution of form in metal-organic frameworks. Nature Communications **2017**, *8*, 1-8.
37. Cohen, S. M.; Postsynthetic Methods for the Functionalization of Metal-Organic Frameworks. Chemical Reviews **2012**, *112*, 970-1000.
38. Tanabe, K. K.; Cohen, S. M.; Postsynthetic modification of metal-organic frameworks – a progress report. Chemical Society Review **2011**, *40*, 498-519.
39. McKinstry, C.; Cussen, E. J.; Fletcher, A. J.; Patwardhan, S. V.; Sefcik, J.; Effect of Synthesis Conditions on Formation Pathways of Metal-Organic Framework (MOF-5) Crystals. Crystal Growth and Design **2013**, *13*, 5481-5486.

Chapter 2: Synthesis of a Bifunctionalizable MOF

Introduction

Metal-organic framework materials have an exceptional history regarding synthetic procedures or premeditated synthetic methodology. As discussed earlier, the core of MOF synthesis is a *de novo* approach known as solvothermal synthesis. MOF chemists have developed strategies to synthesize frameworks that previously were difficult to construct. These strategies of MOF synthesis include novel methods such as PSM,[1] post-synthetic exchange (PSE),[2] solvent assisted ligand exchange (SALE),[3] and many more. The idea of exploring new synthetic strategies is to open pathways to develop MOFs with multiple functions which can be used for various objectives while remaining crystalline and porous.

Strategy

Our goal was to make a MOF that could be tailored to unlock new methods of MOF synthesis by creating a blueprint mixed-ligand MOF that has multifunctionalization potential: large pores, uniform in nature, as well as orthogonally functionalizable.[4] First, mixed-ligand frameworks can be made with commercially available ligands or pre-synthesized ligands. We would like to have ligands with "free" functional groups that can be functionalized further through PSM reactions.[5] Second, we wanted a MOF with large pores for application studies or usage. However, pore space availability is highly contingent on the avoidance of catenation, the self-interpenetration of MOF pores (Figure 1).[7]

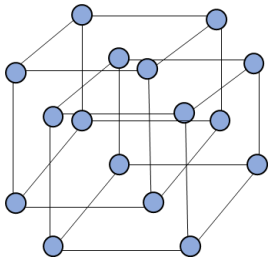

Figure 1. A schematic diagram of MOF catenation (self-interpenetration).

Third, we wanted a MOF that was uniform in nature so that we had predictable chemical processes that occur within and/or on the surface of the MOF.[6] Last, we wanted to make an orthogonally functionalizable MOF so that we could have selective reactivity of functional groups for the MOF. This allows specific reactions to occur for application-based usage**.** For this chemistry to work, we must have the space to do it. With these ideas in mind, we attempted two simultaneous methods to achieve this MOF.

Attempt 1: Synthesis of a Functionalizable MOF with a Pre-Synthesized Ligand

The first pathway involves two unique ligands (Figure 2), a pre-synthesized "octopus" type ligand (L1) to be solvothermally mixed with a commercially available ligand - meso-α,β-di(4-pyridyl) glycol (DPG). Zinc nitrate hexahydrate is our chosen metal source as well as dimethylformamide (DMF) for the solvent.

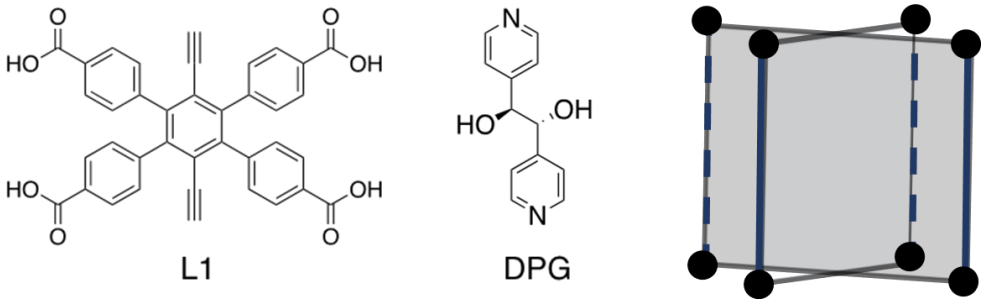

Figure 2. Ligands of choice L1 and DPG with a predicted framework unit cell.

We selected L1 as our *xy* plane ligand because its large size leads to large pores and its alkyne substitution prevents catenation. Additionally, the alkyne group can be reacted with azide groups in a very specific [3+2] cycloaddition. DPG, a dipyridyl molecule, would be our *z*-axis ligand. This ligand acts as the pillar of our molecular "building" and has two alcohol functional groups that have orthogonal reactivity to the alkyne. Zn^{2+} was our chosen metal source because its known participation in the formation of pillared paddle-wheel MOFs.[8, 28]

The synthesis of L1 (Scheme 5) proved to be time consuming and difficult to complete. Steps 1-3 were achieved relatively quickly and with minimal difficulty.[9] However, the di-substitution of alkynes from step 4 via a sonograshira cross-coupling proved to be a tremendous roadblock. This catalyzed reaction allows its user to substitute halogens, in our case bromines, for alkynes.[10-16] We wanted to place the alkynes on the 1 and 4 positions of our central aromatic ring. The sonograshira cross-coupling was attempted many times using different catalysts and reaction conditions, with no success.

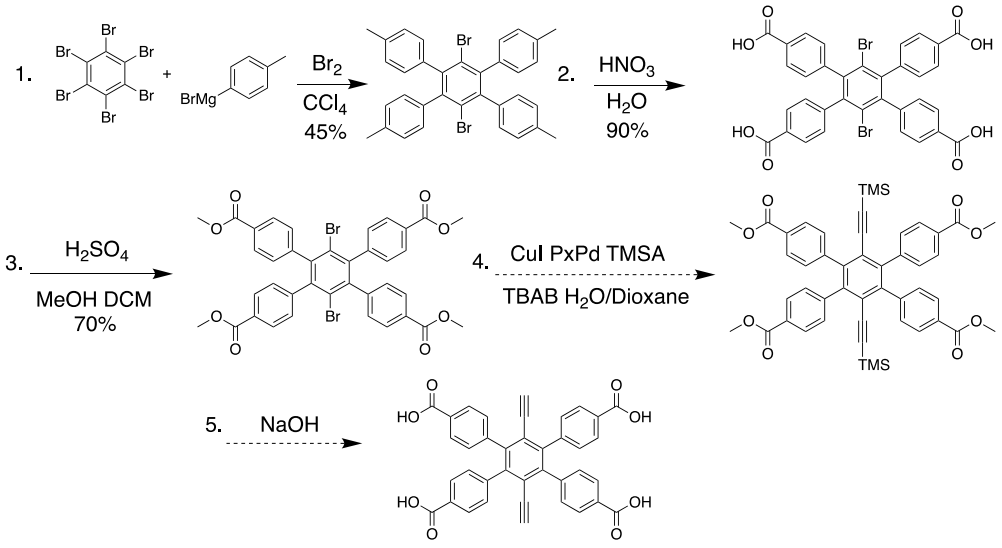

Scheme 5. Synthesis of L1.[9]

A problem for this process is the steric effects that may render the attempts of step 4 unsuccessful. Perhaps a different approach could have been taken at this point, however, the amount of time and effort at step 4 called for a turn of focus onto a project that provided the same end goal.

Attempt 2: Synthesis of a Mixed Ligand MOF - KSU-1

We attempted to synthesize a mixed ligand MOF solvothermally from commercially available materials: Zinc nitrate hexahydrate, 2-aminoterepthalic acid (BDC-NH_2), DPG, and DMF as our solvent (Scheme 6). BDC-NH_2 is a diacid molecule that acts as our *xy* plane ligand and like L1, also has a chelation effect with Zn^{2+}, but with two carboxylic acid functionalities instead of four.

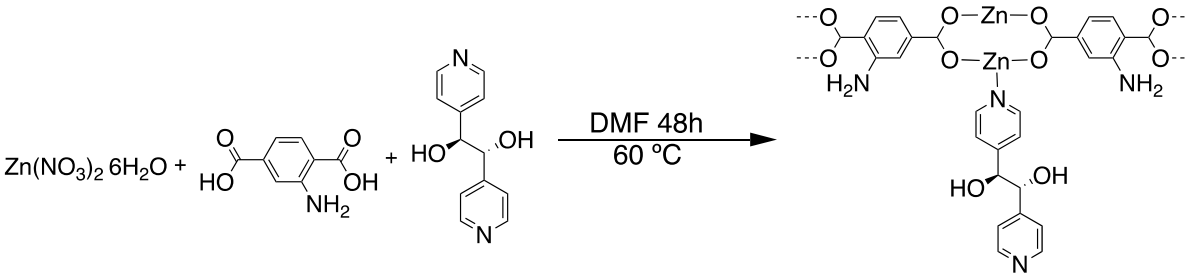

Scheme 6. Synthetic route for KSU-1.

After setting aside a vial containing the mixture for KSU-1 at room temperature, we noticed a mixture of IRMOF-3 orange cubic crystals and a yellow prism like crystal, KSU-1 (Figure 3).[17] We then sent off that sample to collect single crystal x-ray diffraction data and received a kagome (hexagram) lattice structure (Figure 4). We were pleased to obtain this structure because it had large pores, with independently functionalizable groups (amines and hydroxyls) in well-defined positions. Our objective at that time was to collect the yellow prism crystals from the orange cubic crystals.

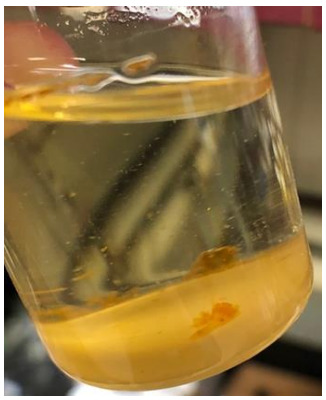

Figure 3. A mixture of KSU-1 yellow prismatic crystals and IRMOF-3 orange cubic crystals.

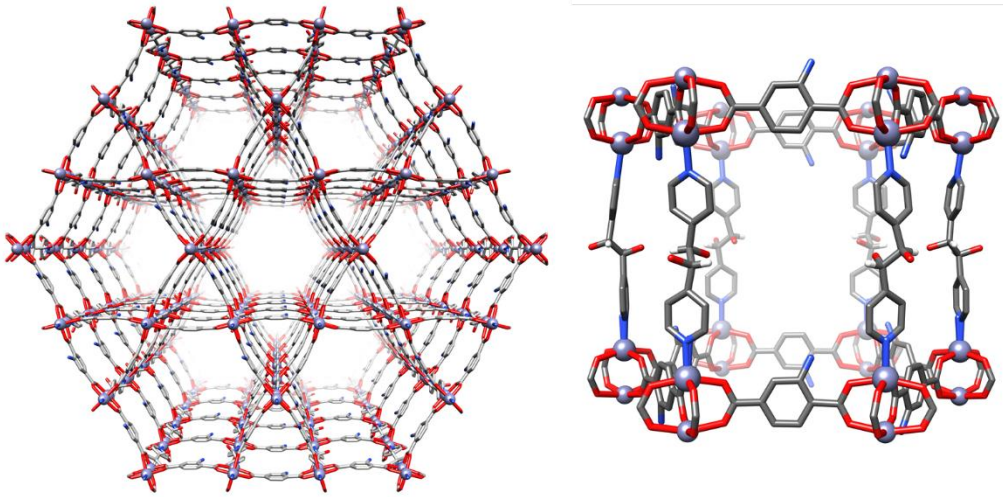

Figure 4. Left: a top view of KSU-1 down the c-axis. Right: a single network unit view of KSU-1.

The synthetic procedure for KSU-1, at this point, had undesirable conditions and formed unwelcome products. Our next objective to synthesize KSU-1 in a pure phase was set in motion. Our knowledge of solvothermal synthesis made it clear that obtaining a pure phase

KSU-1 would present many challenges due to the potentiality of various reaction conditions in which the crystals could grow.

Growing and Purification Challenges of KSU-1

The growing and purification process for MOFs is challenging, making it the largest hurdle in our synthetic strategy. MOF growth and purification face synthetic problems of mixed crystal phases[18] and the formation of impurities due to ligand insolubility, temperature variation, concentration of materials, molar ratios, and growing environment.[19] Various impurities can appear in the reaction process if proper conditions are not met for MOF.

First, the main problem we needed to address was the mixture of KSU-1 and IRMOF-3. These MOFs differ in chemical make-up ($Zn_2(BDC\text{-}NH_2)_2(DPG)$ and $Zn_4O(BDC\text{-}NH_2)_3$ respectively), color, and shape. Since MOFs grow in certain surroundings under solvothermal conditions we had to explore physical and chemical influences in the growth environment of KSU-1 to eliminate the possibility of growing IRMOF-3.[20]

Second, ligands undissolved in the reaction mixture will not play a role in a desired synthesis for the framework crystallization.[21] Our first challenge during this synthesis was the solubility of DPG. We noticed that the DPG was highly insoluble at room temperature in DMF, leading to the formation of several impurities that would fall out of the solution during crystal formation. We found that an optimal way of growing KSU-1 was to first dissolve DPG and zinc nitrate hexahydrate until they became a clear solution at 60 °C then adding a solution of $BDC\text{-}NH_2$ in DMF. We immediately took notice of the purity increase that came from this change in our procedure.

Third, temperature effects can lead to changed topology based on the physical properties influenced during crystallization. Metal-organic frameworks are known to grow in a wide range of temperatures and have different crystal structures because of this influence.[15] The formation of KSU-1 is optimally done at 60 °C to afford its kagome lattice. Attempts at higher temperatures specifically 80 °C and 100 °C led to the formation of IRMOF-3, which is typical of its growth temperature.[21] KSU-1 grows in an interesting way because crystal formation takes place in larger quantities after heating has taken place and letting the solution rest at room temperature for 24 hours. Kagome lattice MOFs, as previously investigated by Furukawa *et al.*, are known to begin nucleation at lower temperatures after heating and crystallize further into these networks at room temperature, backing our interesting discovery for our MOF.[22]

Fourth, the concentration of starting materials plays a part in desired MOF formation by balancing metal and ligand amounts in solution for the formation of frameworks.[23] Frameworks can grow at various concentrations. The concentration effects of our starting materials became vital a component in the synthesis of KSU-1. During the first attempts at synthesis, the metal and ligands would not form any type of crystals at high concentrations (relative to the actual concentrations of materials used to make KSU-1) or continued to form a mixture of KSU-1 and IRMOF-3. We tried using reagent concentrations such as 10 mM, 15 mM and 20 mM. The concentrations that did grow KSU-1 crystals are 3.2 mM, 5 mM, and 5 mM (Zn: BDC-NH_2: DPG). These growth parameters were at very low concentrations, a surprising feat.

Fifth, crystalline materials are highly ordered, well defined, and grow at specific mole ratios to fulfill certain structures. Since MOFs are crystalline materials, they too have mole ratios between the metal and the ligands to arrange into their respective constructs.[24] The mole ratio for KSU-1 growth to occur is 0.32:0.50:0.49 mmol (Zn:BDC-NH_2:DPG) stoichiometric ratio, but interestingly forms a 2:2:1 unit.

Upon discovering these pure phase conditions to grow KSU-1, we finally had nice yellow prism like crystals without any IRMOF-3 or other impurities (Figure 5).

Figure 5. Pure phase KSU-1 yellow prismatic crystals. White powder is DPG that crashes out of solution. It can be removed by several DMF washes.

From the single-crystal X-ray data we obtained of the material which we compared to the PXRD of our as-synthesized MOF with a hexagonal pore of 2 nm in length and a secondary pore of 1 nm in length. We found a nice alignment of peaks, justifying our MOF synthesis route. However, the PXRD of the as-synthesized KSU-1 is not an ideal spectra that we would like to have because of the formation of smaller peaks that are not in the simulation. An interesting observation is that the relative intensities of the patterns are of not of equal

height. The intensities can vary based on the amount of pre-heating time for kagome structured MOFs.[22]

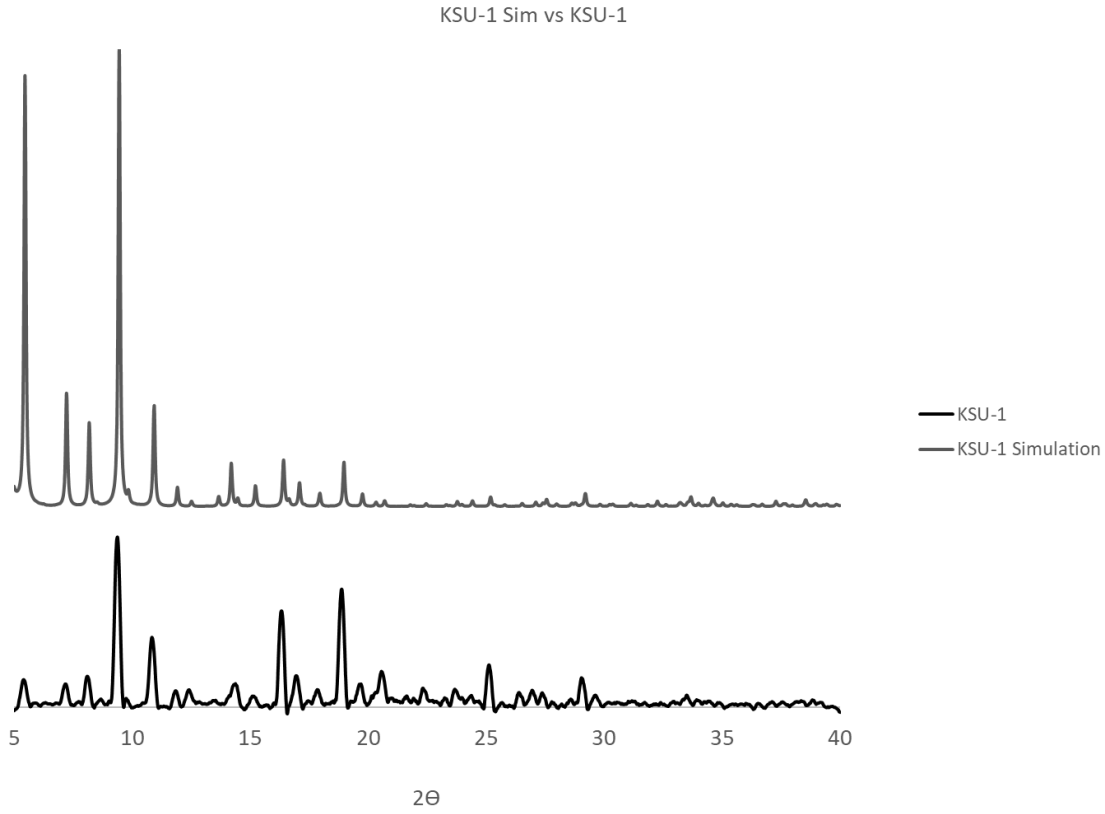

Figure 6. Single crystal structure of KSU-1 top and side view (top) and a powder x-ray diffraction of synthesized KSU-1 with its simulated pattern (bottom). The as synthesized PXRD

MOFs sometimes will need to have their solvent evacuated from their pores. This is done investigate their porosity. Some solvents have higher surface tensions and tend to "stick" to the frameworks more than others. This phenomenon is dangerous to MOF integrity because the solvent molecules with high surface tension are being pulled from the framework while being very physically attached. The can lead to MOF disassembly and likely loss of its crystallinity upon being evacuated. Therefore, it is pertinent to exchange

out these solvents with ones of lower surface tension, as demonstrated by Matzger *et al.*[26] This became crucial for our characterizations.

After PXRD of the pure phase KSU-1 was done, ^{1}H NMR (Figure 7) spectra were collected of pure phases of KSU-1 digested in D_6DMSO/D_2SO_4. The spectra of KSU-1 has a stoichiometric ratio of 2:1 BDC-NH_2 to DPG. Figure 7 displays NMR spectra of as-synthesized KSU-1 compared to the starting ligands.

The peaks indicative of the two BDC-NH_2 ligands are a double, singlet, and a doublet in the aromatic region between 7.0 ppm and 8.0 ppm. The DPG protons are a singlet from two aliphatic protons at ~5.0 ppm and two doublets from symmetrical aromatic protons at 8.0 ppm and 8.9 ppm.

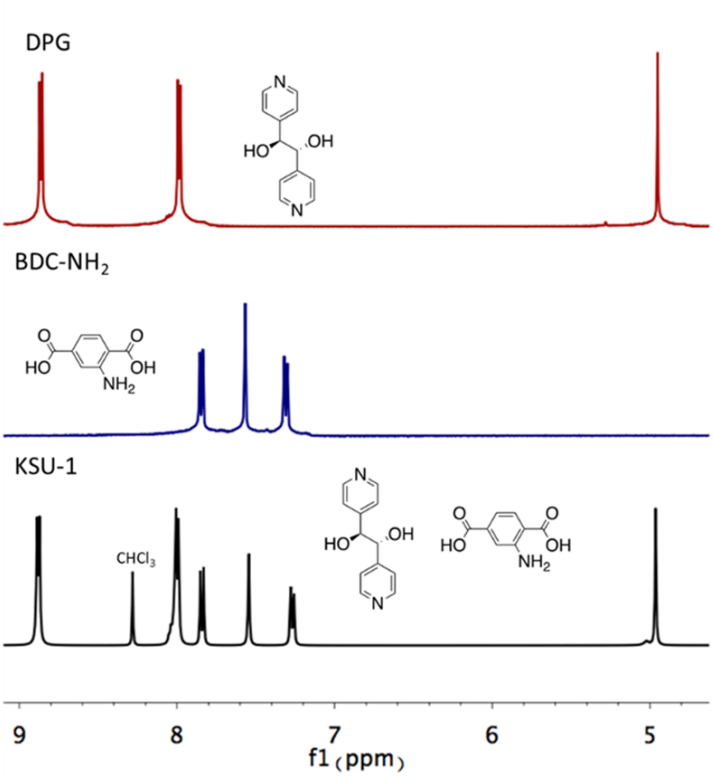

Figure 7. ^{1}H NMR of KSU-1 (black) compared to individual BDC-NH2 (blue) and DPG (red) spectra to confirm their presence in the MOF.

Thermal studies on MOFs are a vital component to their characterization to display their porous nature as well as their thermal stability at high temperatures – characteristics that are common among MOFs.[30-34] Thermogravimetric analysis (TGA) done on KSU-1 confirmed its porous nature and thermal stability at high temperatures. Figure 8 shows the relation of KSU-1 in its as-synthesized form and is compared to its evacuated form, as well as a re-solvated form. The as-synthesized TGA is to show the natural porosity and thermal stability of KSU-1. The evacuated and re-solvated trials are done to show if KSU-1 can maintain its porous nature after being subjected to a vacuum environment.

The TGA data of the as-synthesized MOF shows DMF solvent loss at about 50% of the total mass, at the boiling point of DMF (~153 °C), confirming the large pores that the MOF contains as well as the thermal stability of the MOF holding up until decomposition occurs at about 350°C. Upon evacuation, the expected curve of the data shows the complete loss of solvent. When the sample is re-solvated after evacuation, the MOF maintains some of its porosity as there is still solvent loss from the pores at around 30% of the total mass of the sample. The TGAs done on KSU-1 help confirm our expectations of porosity from the single crystal data that we received in that we have a porous MOF that is thermally stable.

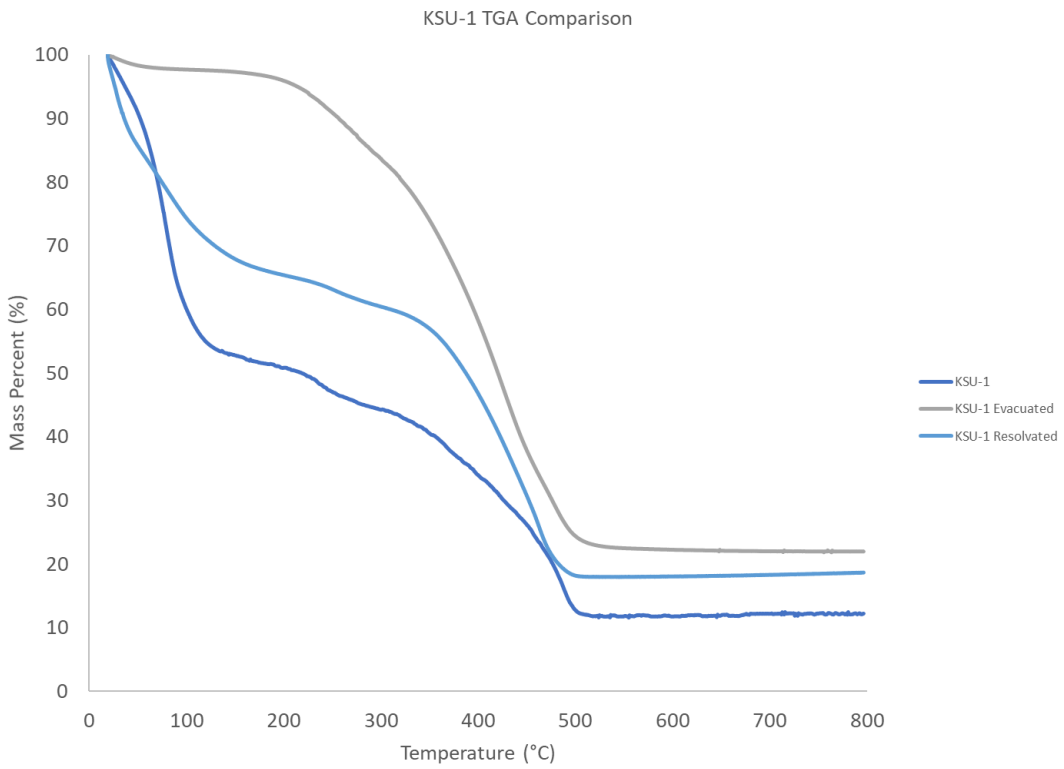

Figure 8. TGA of KSU-1 as synthesized, KSU-1 evacuated, and KSU-1 re-solvated.

Conclusion

A mixed-ligand metal-organic framework known as KSU-1 has successfully been synthesized solvothermally using commercially available materials $Zn(NO_3)_2$ $6H_2O$, BDC-NH_2, DPG, and DMF. The synthesis afforded yellow prismatic crystals. Upon receiving single crystal data, our crystal is a mesoporous kagome structured framework with large, unexpected pores. This MOF provided the large pores sizes and independently modifiable functionalities required for the independent postsynthetic modification, allowing us to demonstrate out MOF bifunctionalization and eventually an orthogonally functionalized MOF.

Experimental

General synthesis of L1 – step 1.[9] 100 mL of *p*-tolylmagnesium bromide (1M in THF) is added to a round bottom flask containing 5 g of hexabromobenzene in a glove box under nitrogen atmosphere. The mixture was stirred at room temperature for 15 hours and became a grey suspension. The reaction was placed in an ice bath where a mixture of 7 mL of bromine and 60 mL of CCl_4 are added dropwise to the reaction while stirring. The reaction underwent stirring for 1.5 hours followed by the addition of 50 mL of HCl (6 M). 2 g of yellow solid was filtered and washed with methanol then weighed.

General synthesis of L1 – step 2.[9] 200 mg of product from step 1 is placed in a 100 mL Teflon vessel where a mixture of 8:2 H_2O to concentrated HNO_3 is added. The vessel is placed in a oven at 180 ^oC for 18 hours. After cooling to room temperature, the product is filtered and washed with H_2O and a 3:7 mL ratio of THF and $CHCl_3$ mixture. The product is set out to dry then weighed.

General Synthesis of L1 – step 3.[9] 200 mg from step 2 is weighed out and placed in a 250 mL round bottom flask with 40 mL of methanol and 40 mL of DCM in the presence of sodium sulfate and molecular sieves. The mixture is stirred under the addition of 4 mL of H_2SO_4. The reaction is stoppered and allowed to stir for 48 hours. The reaction is then quenched with a saturated sodium bicarbonate solution, extracted with a separatory funnel and dried over magnesium sulfate.

Synthesis of KSU-1. $Zn(NO_3)_2 \cdot 6H_2O$ (95.2 mg, 0.32 mmol), DPG (106 mg. 0.49 mmol), and DMF (80 mL) were combined in a 500 mL Florence flask. The flask was heating to 60 °C in a 500 mL heating block until the solution becomes clear. A solution of BDC-NH_2 (90.6 mg, 0.50 mmol) in DMF (20 mL) is added, and the flask if left to heat at 60

°C. After 48 h, the flask is removed from the heating block and left at room temperature for 48 h. Pale yellow crystals (40 mg, 35% yield) of the product were collected and placed in an exchange thimble inside of a 20 mL scintillation vial. The MOF crystals are subjected to undergo solvent exchanges with fresh DMF 3 times for 15 minutes each on a Corning LSE Low Speed Orbital Shaker. The crystals then undergo solvent exchanges with $CHCl_3$ 5 times and then hexanes 5 times each for 15 min each on the shaker. The MOF crystals are then isolated via vacuum filtration and then stored under vacuum at 80 °C.

Characterization

Powder X-ray diffraction (PXRD) patterns were recorded on a Bruker AXS D2 Phaser SSD160 diffractometer using nickel-filtered Cu Kα radiation (λ = 1.5418 Å) over a range of $5° < 2\theta < 40°$ in 0.1° steps with a 1-s counting time per step. Samples were collected from the bottom of the reaction vial as a thick suspension in DMF and spread on a Si-Einkristalle plate immediately before PXRD measurements. Given the high boiling point of DMF, the crystals never dry out during the PXRD measurement.

^{1}H NMR spectra were recorded on a Varian 400MHz NMR spectrometer (400 MHz for ^{1}H). NMR chemical shifts were reported in ppm against residual solvent resonance as the internal standard ($\delta(d_6DMSO) = 2.5$ ppm). Samples of MOF (~ 2 mg) were transferred into an NMR tube and D_2SO_4 (0.01 mL, 98% w/w in D_2O) was added. The tubes were capped and sonicated until all the solid was dissolved (~ 1 min).

Thermogravimetric analysis (TGA) was performed on a TGA-Q50 interfaced with a PC using TA Universal Analysis software. Samples were heated at a rate of 10 ºC/min under

a nitrogen atmosphere. Modified samples were extensively rinsed with DMF prior to analysis. Evacuated samples are exchanged with hexanes prior to evacuation to avoid pore collapse. Re-solvated samples are first exchanged with hexanes, evacuated, then re-solvated in DMF prior to analysis.

Chapters References

1.Zons, T. V.; Brokmann, L.; Lippke, J.; PreuBe, T.; Hulsmann, M.; Schaate, A.; Behrens, P.; Godt, A.; Postsynthetic Modification of Metal-Organic Frameworks through Nitrile Oxide-Alkyne Cycloaddition. Inorganic Chemistry **2018**, *57*, 3348-3359.

2. Taddei, M.; Wakeham, R. J.; Koutsianos, A.; Andreoli, A.; Barron, A. R.; Post-Synthetic Ligand Exchange in Zirconium-Based Metal-Organic Frameworks: Beware of the Defects. Angewandte **2018**, *57*, 11706-11710.

3. Lalonde, M. B.; Mondlock, J. E.; Deria, P.; Sarjeant, A. A.; Al-Juaid, S. S.; Osman, O. I.; Farha, O. K.; Hupp, J. T.; Selective Solvent-Assisted Linker Exchange (SALE) in a Series of Zeolitic Imidazolate Frameworks.

4. Zhao, Y.; Emerging Applications of Metal-Organic Frameworks and Covalent Organic Frameworks. Chemistry of Materials **2016**, *28*, 8079-8081.

5. Gadzikwa, T.; Farha, O. K.; Mulfort, K. L.; Hupp, J. T.; Nguyen, S. T.; A Zn-based, pillard paddlewheel MOF containing free carboxylic acids via covalent post-synthesis elaboration. Chemical Communications **2009**, *25*, 3720-3722.

6. Wu, C. D.; Zhao, M.; Incorporation of Molecular Catalysts in Metal-Organic Frameworks for Highly Efficient Heterogeneous Catalysis. Advanced Materials **2017**, *14*, 1605446-1605446.

7. Farhar, O. K.; Malliakas, C. D.; Kanatzidis, M. G.; Hupp, J. T.; Control over Catenation in Metal-Organic Frameworks via Rational Design of the Organic Building Block. Journal of American Chemical Society **2010**, *132*, 950-952.

8. Ma, B.; Mulfort, K. L.; Hupp, J. T.; Microporous Pillarad Paddle-Wheel Frameworks Based on Mixed-Ligand Coordination of Zinc Ions. Inorganic Chemistry **2005**, *44*, 4912-4914.

9. Mulfort, K. L.; Farha, O. K.; Stern, C. L.; Sarjearnt, A. A.; Hupp, J. T.; Post-Synthesis Alkoxide Formation Within Metal-Organic Framework Materials: A Strategy for Incorporating Highly Coordinatively Unsaturated Metal Ions. Journal of American Chemical Society **2009,** *131*, 3866-3868.

10. Schilz, M.; Plenio, H.; A Guide to Sonogashira Cross-Coupling Reactions: The Influence of Substituents in Aryl Bromides, Acetylenes, and Phosphines. Journal of Organic Chemistry **2012**, *77*, 2798-2807.

11. Wang, X.; Song, Y.; Qu, J.; Luo, Y.; Mechanistic Insights into the Copper - Cocatalyzed Sonogashira Cross-Coupling Reaction: Key Role of an Anion. Organometallics **2017**, *36*, 1042-1048.

12. Negishi, E.; Qian, M.; Zeng, F.; Anatasia, L.; Babinski, D.; High Satisfactory of Alkenyl Halides via Pd-Catalyzed Cross-Coupling with Alkynylzincs and Its Critical Comparison with the Sonogashira Alkynylation. Organic Letters **2003**, *5*1597-1600.

13. Santandrea, J.; Bedard, A.; Collins.; Cu(I)-Catalyzed Macrocycloc Sonogashira-Type Cross Coupling. Organic Letters **2014**, *16*, 3892-3895.

14. Li, N.; Lim, R. K. V.; Edwardraja, S.; Lin, Q.; Copper-Free Sonogashira Cross-Coupling for Functionalization of Alkyne-Encoded Proteins in Aqueous Medium and in Bacterial Cell. Journal of American Chemical Society **2011**, *133*, 15316-15319.

15. Pu, X.; Li, H.; Colacot, T. J.; Heck Alkynylation (Copper-Free Sonogashira Coupling) of Aryl and Heteroaryl Chlorides, Using Pd Complexes of t-Bu_2(*[*-

$NMe_2C_6H_4$)P: Understanding the Structure-Activity Relationships and Copper Effects. Journal of Organic Chemistry **2013**, *76*, 568-581.
16. Pohida, K.; Maloney, D. J.; Mott, B. T.; Rai, G.; Room-Temperature, Copper-Free Sonogashira Reactions Facilitated by Air-Stable, Monoligated Precatalyst [DTBNnP] Pd(crotyl)Cl. American Chemical Society Omega **2018**, *3*, 12985-12988.
17. Rowsell, J. L. C.; Yaghi, O. M.; Metal-organic frameworks: a new class of porous materials. Microporous and Mesoporous Materials **2004**, *73*, 3-14.
18. Guillerm, V.; Kim, D.; Eubank, J. F.; Luebke, R.; Liu, X.; Adil, K.; Lah, M. S.; Eddaoudi, M.; A Supermolecular Building Approach for the Design and Construction of Metal-Organic Frameworks. Chemical Society Review **2014**, *43*, 6141-6172.
19. Hendon, C. H.; Rieth, A. J.; Korzynski, M. D.; Dinca, M.; Grand Challenges and Future Opportunities for Metal-Organic Frameworks. ACS Central Science **2017**, *3*, 554-563.
20. Chen, F.; Bai, D.; Wang, Y.; He, M.; Gao, X.; He, Y.; A pair of polymorphous metal-organic frameworks based on an angular siisophthalate linker: synthesis, characterization and gas adsorption properties. Dalton Transactions **2018**, *47*, 716-725.
21. Karagiaridi, O.; Bury, W.; Sarjeant, A. A.; Hupp, J. T.; Farha, O. M.; Synthesis and Characterization of Functionalized Metal-Organic Frameworks. Journal of Visualized Experiments **2014**, *91*, 1-9.
22. Kondo, M.; Takashima, Y.; Seo, J.; Kitagawa, S.; Furukawa, S.; Control over the nucleation process determines the framework topology of porous coordination polymers. Crystal Engineering Communication **2010**, *12*, 2350-2353.
23. Zhou, H.; Sun, Y.; Recent progress in the synthesis of metal-organic frameworks. Science and Technology of Advanced Materials **2015**, *16*, 1-11.
24. Seetharaj, R.; Vandana, P.V.; Arya, P.; Mathew, S.; Dependence of solvents, pH, molar ratio, and temperature in tuning metal organic framework architecture. Arabian Journal of Chemistry **2016**, 2-21.
25. Poddar, T. K.; Sirkar, K. K. Henry's Law constant for Selected Volatile Organic Compounds in High-Boilinb Oils. Journal of Chemical Engineering **1996**, *41*, 1329-1332.
26. Ma, J.; Kalenak, A. P.; Wong-Foy, A. G.; Matzger, A. J.; Rapid Guest Exchange and Ultra-Low Surface Tension Solvents Optimize Metal-Organic Framework Activation. Angewandte Chemie International Edition **2017**, *56*, 14618-14621.
27. Zhou, K.; Chaemchuen, S.; Wu, Z.; Verpoort, F.; Rapid room temperature synthesis forming pillard metal-organic frameworks with Kagome net topology. Microporous and Mesoporous Materials **2016**, *239*, 28-33.
28. Li, J.; Peng, Y.; Liang, H.; Yu, Y.; Xin, B.; Li, G.; Shi, Z.; Feng, S.; Solvothermal Synthesis and Structural Characterization of Metal-Organic Frameworks with Paddle-Wheel Zinc Carboxylate Clusters and Mixed Ligands. European Journal of Inorganic Chemistry **2011**, *2011*, 2712-2719.
29. Servalli, M.; Ranocchiari, M.; Van Bokhoven, J. A.; Fast and high yield post-synthetic modification of metal-organic frameworks by vapor diffusion. Chemical Communications **2012**, *48*, 1904-1906.
30. Walton, K. S.; Mu, B.; Thermal Analysis and Heat Capacity Study of Metal-Organic Frameworks. Journal of Physical Chemistry **2011**, *115*, 22748-22754.
31. Bae, Y.; Dubbeldam, Nelson, A.; Walton, K. S.; Hupp, J. T.; Snurr, R. Q.; Strategies of Large-Pore Metal-Organic Frameworks by Combined Experimental and Computational Methods. Chemistry of Materials **2009**, *21*, 4768-4777.

Chapter 3: Reductive Amination and Other Postsynthetic Modification Routes to a Bifunctionalized MOF

Introduction

To synthesize our bifunctionalized MOF, two routes of postsynthetic modification were chosen. For our MOF to undergo independent functionalization, the functional groups of the ligands must selectively undergo reactions in which one functionality of a ligand will react fully and the functional group(s) of the other ligand will not. This selectivity was carefully planned around the nucleophilicity of the functional groups in KSU-1, the formation of a new functionality, and the reaction conditions during this process.

Strategy

When developing this two-step PSM strategy, our intention was to do a PSM on our more nucleophilic amine functional group first. PSM reactions on amines in MOFs have been previously reported.[1] The most common PSM reactions for amines includes the formation of amides,[2] ureas,[3] and azides.[4] Our intent for the first PSM pathway was to perform an imine condensation on our amine functional group (Scheme 7) with benzaldehyde, following similar imine condensation reaction conditions found in literature.[5-6] However, this imine condensation reaction was troublesome because of hydrolysis of the product imine and the use of low concentrations.

To combat hydrolysis, we did the reaction in a drier environment using molecular sieves to slow the hydrolyzing effect of the imine. The condensation reaction using benzaldehyde was done at a low concentration, potentially attributing to the lack of imine formation. After the continued struggle with hydrolysis we switched to salicylaldehyde (Scheme 8) hoping that a more stable imine would form and not be as prone to hydrolysis. We also increased the concentration of the aldehyde to promote product formation.

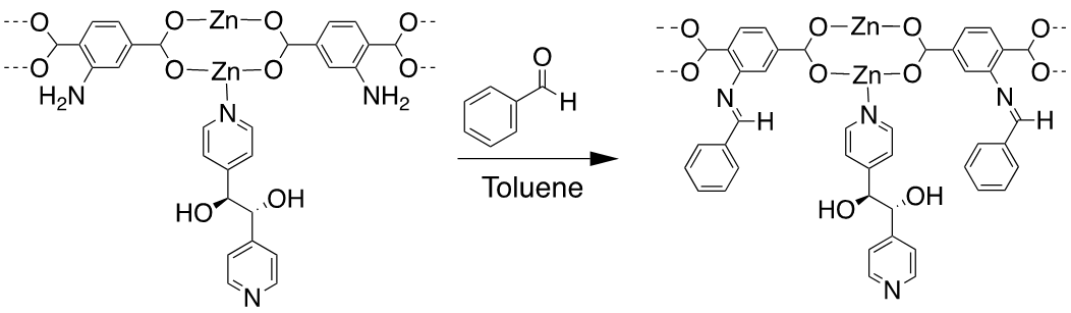

Scheme 7. Imine condensation reaction scheme with benzaldehyde as the chosen aldehyde.

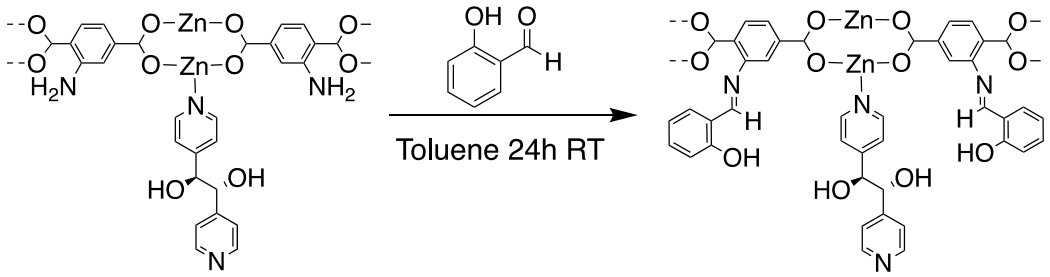

Scheme 8. Salicylaldehyde imine condensation PSM of KSU-1 reaction scheme.

^{1}H NMR of the salicylaldehyde PSM in KSU-1 shows that the imine formed after reacting with our BDC-NH_2 ligand (Figure 9). When the MOF was digested in D_6DMSO and D_2SO_4, hydrolysis of the imine occurred, and we see in the spectra the original MOF components and salicylaldehyde. However, we were able to see the relative ratios reflecting conversion of the amine to the imine. This was good news, but we again ran into trouble with imine hydrolysis when performing a second PSM reaction (the PSM step is discussed later in this chapter) involving succinic anhydride and DPG to form diesters.

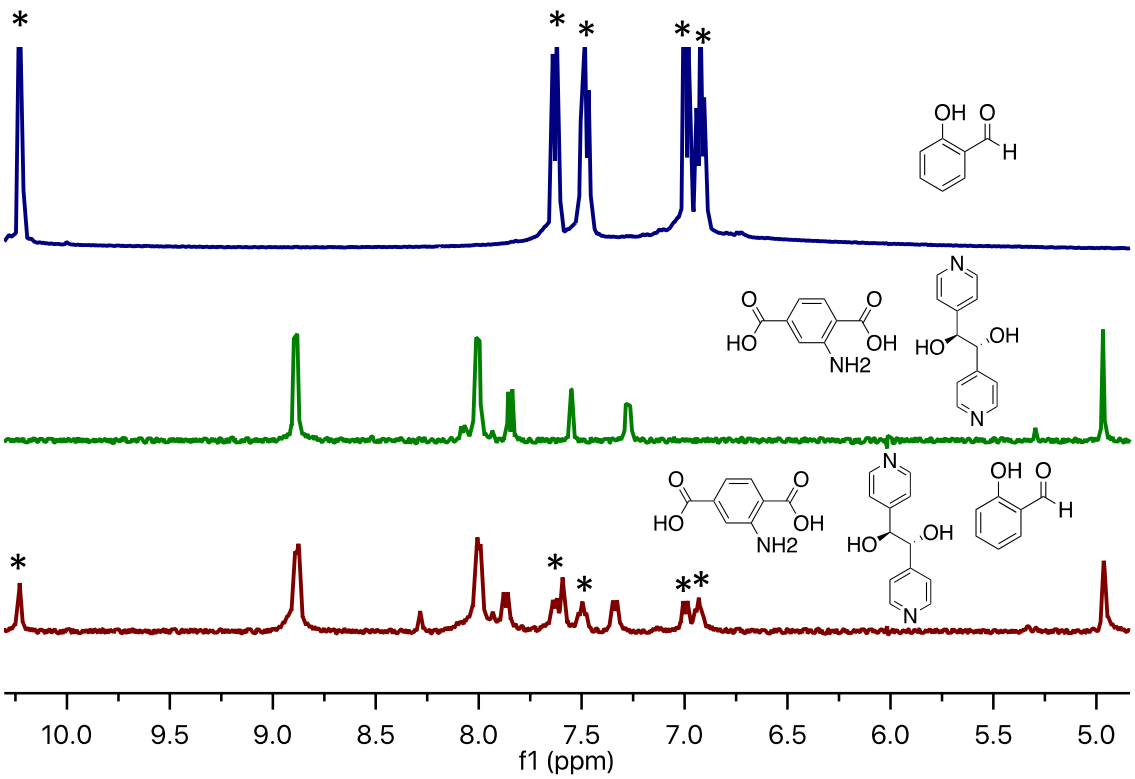

Figure 9. Stacked ^{1}H NMR spectra of imine condensation PSM involving salicylaldehyde on KSU-1.

It appears this reaction had pushed the conversion of the amine into an imine while using the salicylaldehyde as the aldehyde of choice from our NMR spectra. However, we continued to get hydrolysis again and again after the addition of succinic acid in solution during the second PSM step. Since acids can hydrolyze imines, perhaps the hydrolysis of the imine resulted from the presence of succinic acid.

Since the hydrolysis of our imine functional groups kept occurring, we chose a different route to combat this issue. This newly designed PSM pathway (Scheme 9) was chosen to follow the imine condensation reaction with the amine on BDC-NH_2 in KSU-1. We chose reductive amination, which reduces the imine into a secondary amine in the presence of a reducing reagent. Reductive amination is a well-known reaction that is useful because the

resulting secondary amine is inert to hydrolysis. Examples of reductive amination in MOFs are also present in literature giving us cause to perform a reductive amination in KSU-1.[7-20]

Our aldehyde of choice in this reaction was once again benzaldehyde. Our reducing agent used in this reaction was sodium cyanoborohydride ($NaBH_3CN$) in DMF to react with benzaldehyde for three days. Reducing agents such as $NaBH_3CN$, are mild compared to other reducing agents such as sodium borohydride because of the addition of a nitrile electron withdrawing group.[21-23]

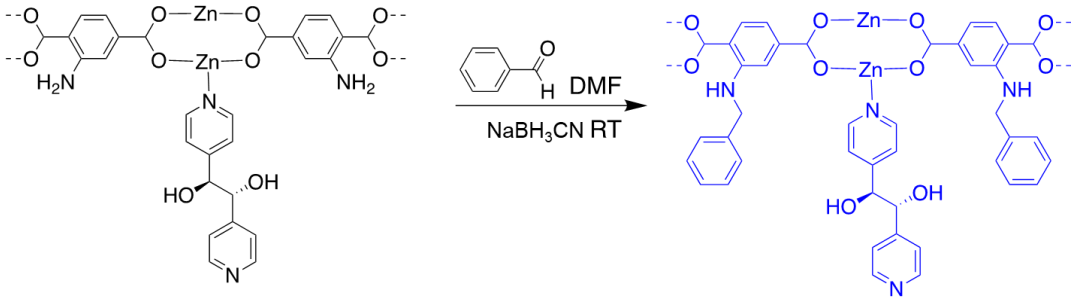

Scheme 9. Reductive Amination of KSU-1 to KSU-1-RA using benzaldehyde, sodium cyanoborohydride in DMF at RT.

The nucleophilic ring opening of succinic anhydride was chosen as our second PSM step (KSU-1-RA to KSU-1-multi). We chose this as our second PSM because of the reactivity of succinic anhydride in the presence of a nucleophile due to ring strain (Scheme 10).[24] The nucleophilic ring opening was chosen to react with the alcohols of DPG to form diesters. This reaction was done at 0.2 M in DMF for two days. If this reaction is done in the presence of a free NH_2 as well as the OH functional groups, it would likely react with both simultaneously thus thwarting the idea of independent functionalization (Scheme 11).

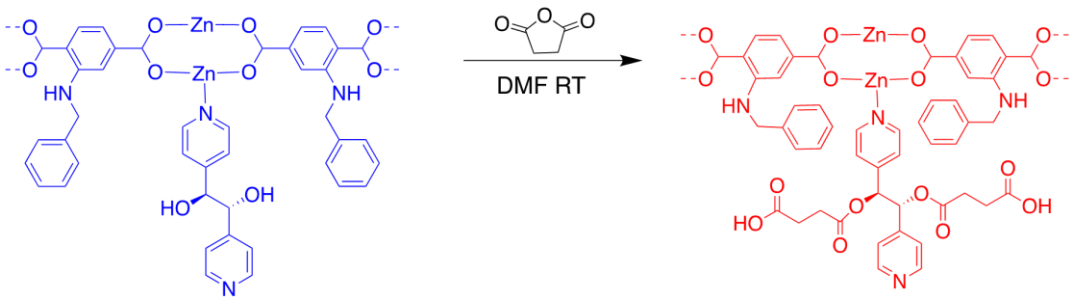

Scheme 10. Nucleophilic opening of succinic anhydride to from KSU-1-multi.[25]

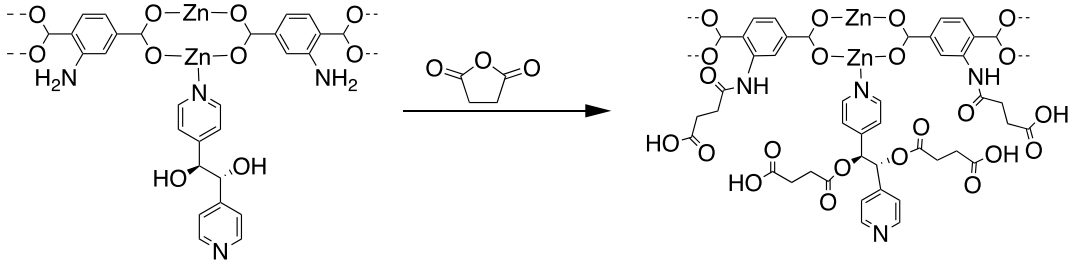

Scheme 11. Example of dependent functionalization on KSU-1 if the PSM reaction pathways are reversed.

Reductive Amination PSM Modification Attempts

The formation of the alkylated MOF KSU-1-RA could be seen in our ^{1}H NMR spectra throughout this process, however, problems persisted during the reductive amination PSM pathway which hindered the progress of our synthesis.

First, the amount of time the reaction took place and concentration of the reagents are a large part of the effectiveness of the reaction. The amount of time the reaction takes place was dependent on the concentrations of the reagents. If the concentration of the reagents were high, the MOF crystals disassembled or deformed from their crystalline nature.

First, ^{1}H NMRs were performed on concentrated samples of KSU-1-RA where the benzaldehyde concentration was high. Figure 10 displays both PSM reactions along with KSU-1. The starting material peaks for the BDC-NH_2 ligands shifted because of the change in the chemical environment of the ligands. We also observed the formation of a new aliphatic peak (~4.5 ppm) coming from the alkylation of the amine and a new aromatic proton peak (~7.35 ppm) from the benzyl groups attached to the aliphatic carbon. The formation of diesters on the alcohols following the digestion of KSU-1-multi in D_6DMSO/D_2SO_4 shows succinic acid after hydrolysis.

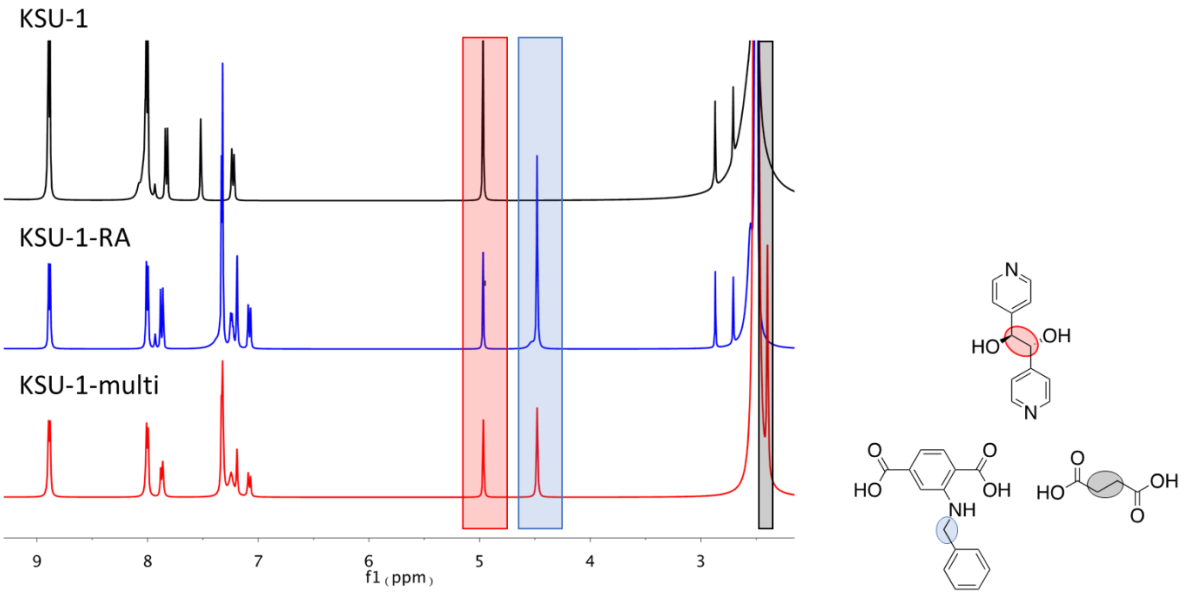

Figure 10. ^{1}H NMR transitions between each PSM step.

At first this was exciting news, however, after several integrations, we noticed that the relative proton ratio of the benzyl amine aliphatic protons was not matching with the expected ratio with the DPG aliphatic protons. Since a secondary amine has a proton source, it is possible for dialkylation to occur and form a tertiary amine from the aldehyde being in such excess.[15] The expected ratio was 4:2 from two secondary amine aliphatic

protons to the aliphatic protons of DPG. The integrations showed a ratio of roughly 6-8:2 leading to our belief that dialkylation of BDC-NH_2 occurred from the concentrated benzaldehyde attempts of reductive amination. Figure 11 shows ^{1}H NMR spectra of several examples of this suspected dialkylation.

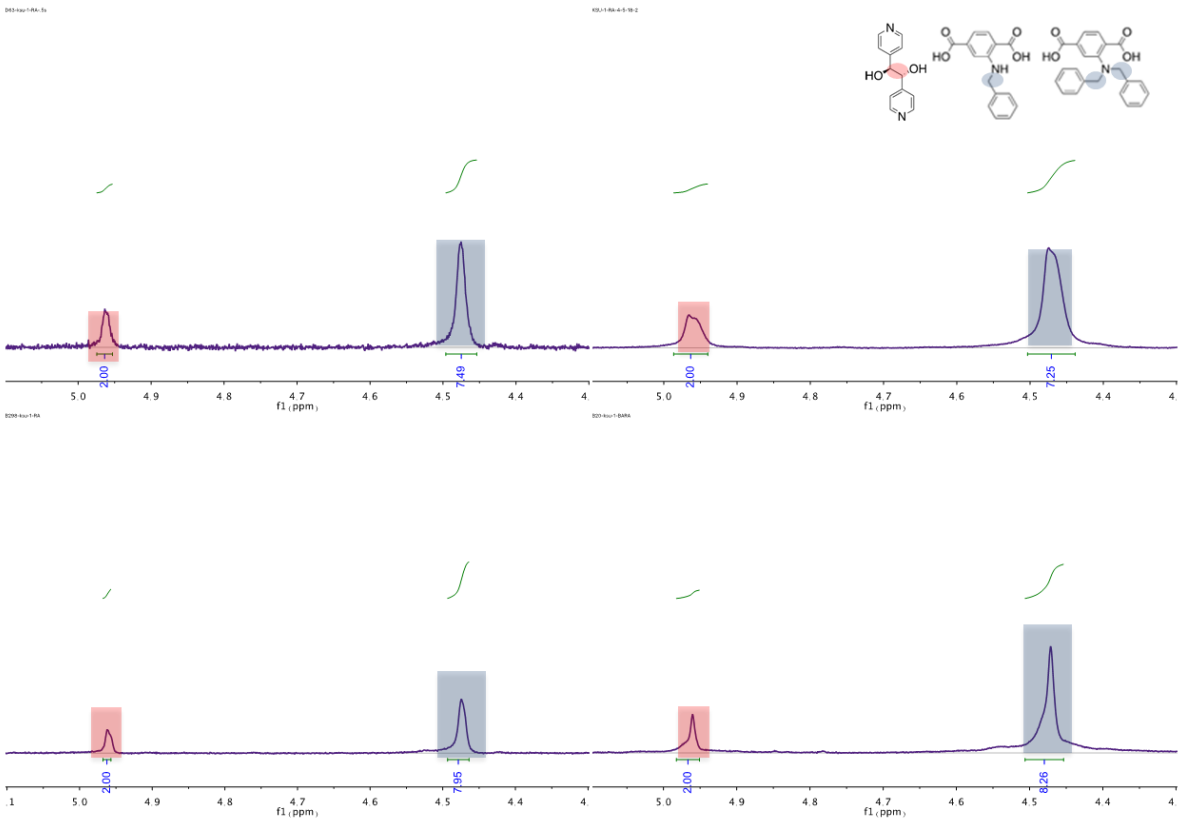

Figure 11. ^{1}H NMR examples of suspected dialkylation of the secondary amine with relative ratios shown to be 6-8:2 in comparison with the aliphatic protons of DPG.

Figure 12 shows PXRD patterns of all PSM steps. The transition between KSU-1 and KSU-1-RA displays the effect the concentrated benzaldehyde had on the crystallinity of the MOF. There was even more of a loss of crystallinity transitioning from KSU-1-RA to KSU-1-multi.

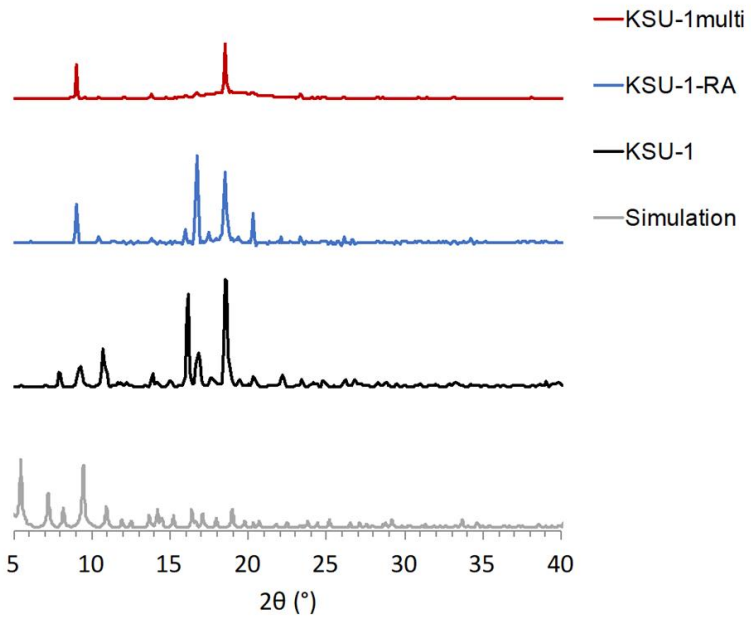

Figure 12. PXRD patterns of KSU-1, KSU-1-RA, KSU-1-multi show the significant loss of crystallinity as each PSM steps proceed.

After attempts with a concentrated benzaldehyde solution, we wanted to try a lower concentrated route for the aldehyde, but we wanted the reducing agent to be at a 1:1 molar equivalent to the aldehyde. With our starting materials at new concentrations as well as using anhydrous DMF as our solvent, we wanted to be sure that this reaction proceeded quicker than the previously reaction. A scale up experiment for reductive amination on KSU-1 was done for a total of six days to track the progression for the formation of the secondary amine and track dialkylation.

Figure 13 shows the ^{1}H NMR progression of the reductive amination for every two days. It appears as if the reductive amination step had worked at a lower concentration of the aldehyde between days one and two. However, dialkylation occurred after day one from over exposure to the aldehyde, an increase in reducing agent, and the use of anhydrous

DMF. Our DPG ligand peaks begin to deform after two days and alkylation appears to proceed further and further as the reaction proceeded. We noticed that the DPG began dissolving out of the MOF after day 2. We also saw the formation of new aliphatic hydrogens began appearing on day six along with the movement the DPG doublets. This led us to believe that alkylation may have occured to our DPG ligands. Although the dialkylation of KSU-1 is not necessarily a problem for our proof of concept of bifunctionalizing a MOF. It was in our best interest to move on to other PSM strategies to avoid the loss of material and improve our chances of increasing yields.

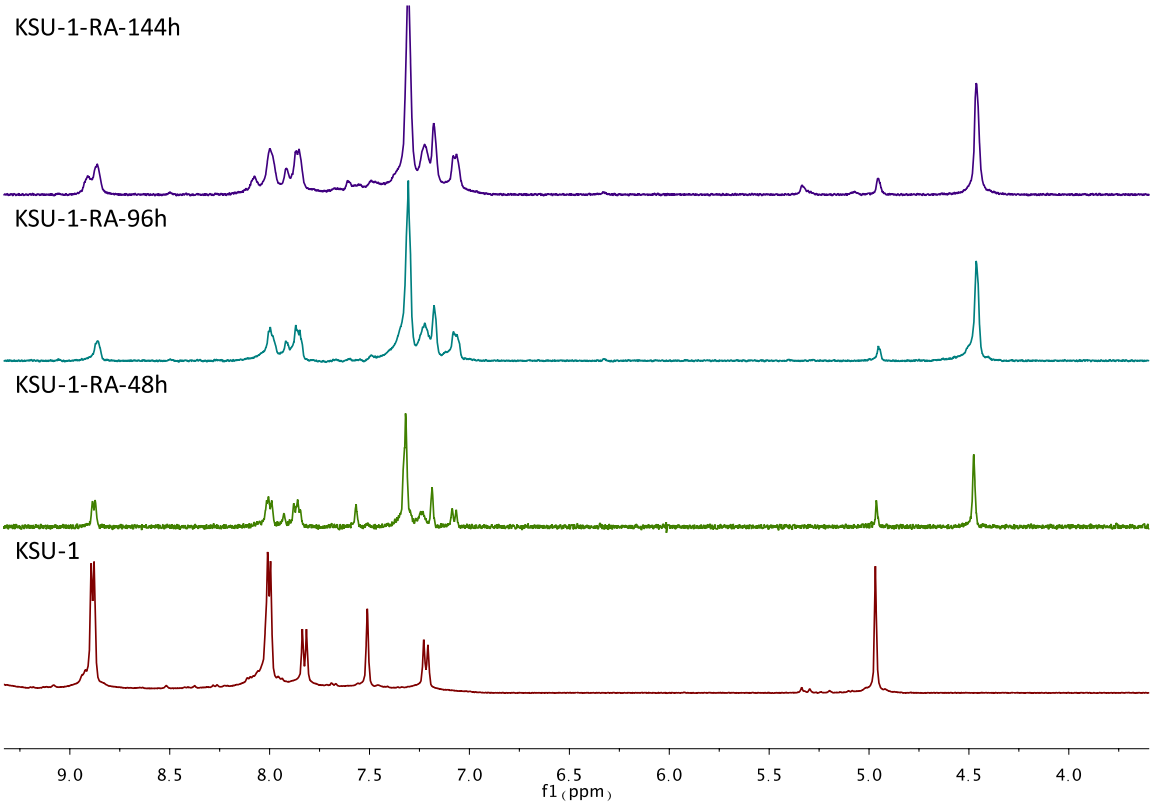

Figure 13. A stack 1H NMR spectra of a six-day reductive amination reaction at lower concentrations of reactants.

A Successful PSM Attempt to bi-functionalize KSU-1 using Anhydrides

After the attempts with these PSM reactions Kanchana Samarakoon successfully used PSM reactions with two anhydride compounds to make KSU-1 bifunctional. She used butyric anhydride and succinic anhydride (Scheme 12). This combination of PSM steps worked by limiting the loss of material from minimal concentrations of reagents. The material also maintains its crystallinity, which is vital for our system to maintain so that when application studies are done in KSU-1 they can be analyzed in a structurally sound environment.

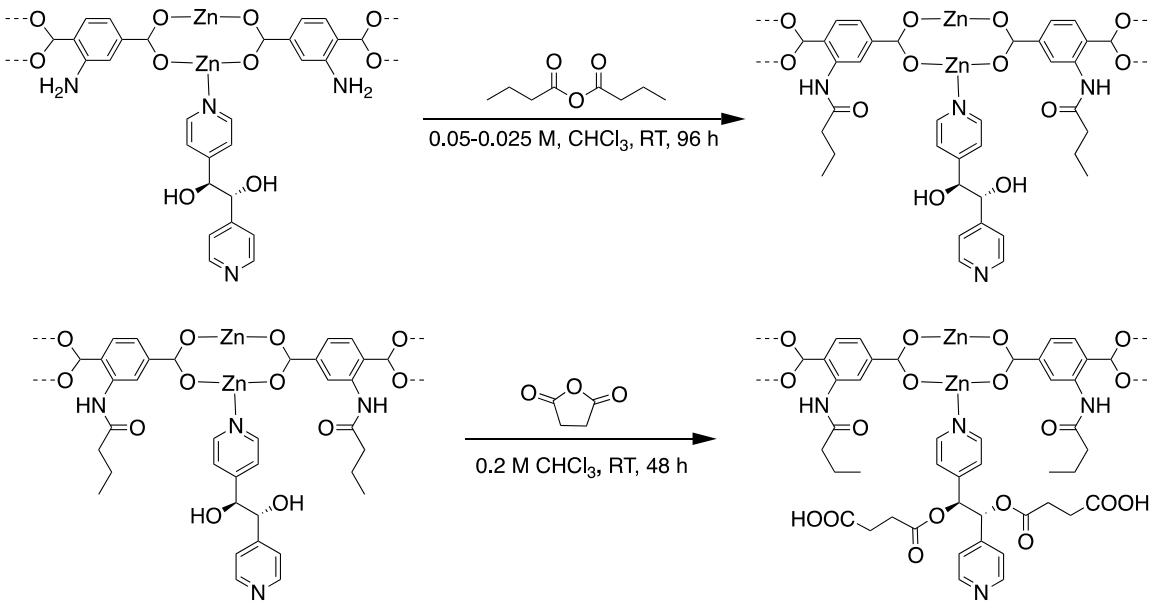

Scheme 12. Successful bi-functionalization of KSU-1 using butyric anhydride and succinic anhydride (work done by Kanchana Samarakoon).[28]

Conclusion

At first, efforts to bi-functionalize KSU-1 to obtain independently functionalized linkers resulted in problems demonstrating this foundational tool. The synthetic strategy of using reductive amination resulted in the loss of material from the high concentration of the aldehyde as well as harshness of the reducing agent. At different concentrations the conversion of the primary amine had either formed secondary amines or a mixture with tertiary amines. Although the reductive amination strategy did work, we chose different synthetic routes to maintain the structural integrity of the MOF. A synthetic strategy with the use of anhydrides on the linkers has successfully demonstrated, for the first time, the sequential, independent bifunctionalization of a MOF material.

Experimental Data

The general procedure for imine condensation of KSU-1 with benzaldehyde. The MOF samples (~15 mg) were transferred into an exchange thimble, that was placed in a 20 mL scintillation vial. The MOF samples were reacted in 0.014 mL of benzaldehyde (1.4×10^{-4} mol, 0.028 M) in 5 mL of toluene in the presence of 3Å molecular sieves at room temperature for 72 h with continuous mixing on a TYZD-IIII Orbital Shaker. The MOFs are then washed with toluene and then solvent exchanged with CHCl3. The MOFs were subjected to vacuum filtration with CHCl3 washes and air dried for 30 minutes. The MOFs were evacuated in a vacuum oven at 80 °C for solvent removal for characterization.

The general procedure for imine condensation of KSU-1 with salicylaldehyde. The MOF samples (~30 mg) were transferred into an exchange thimble, that was placed in a 20 mL scintillation vial. The MOF samples were reacted in 0.12 mL of salicylaldehyde (0.001

mol, 0.5 M) in 2.2 mL of toluene in the presence of 3Å molecular sieves at room temperature for 24 h with continuous mixing on a TYZD-IIII Orbital Shaker. The MOFs are then washed with toluene and then solvent exchanged with CHCl3. The MOFs were subjected to vacuum filtration with CHCl3 washes and air dried for 30 minutes. The MOFs were evacuated in a vacuum oven at 80 °C for solvent removal for characterization.

The general procedure for the higher concentration of reductive amination of BDC-NH2 – KSU-1-RA. The MOF samples (~30mg) were transferred into an exchange thimble, that was placed in a 20 mL scintillation vial. The MOF samples were reacted in 2 mL of benzaldehyde (0.146 mol, 5M), 0.8 mL of 1M sodium cyanoborohydride in DMF (0.016 mol, 0.2M), and 1.2 mL of DMF in the presence of 3Å molecular sieves at room temperature for 72 h with continuous mixing on a TYZD-IIII Orbital Shaker. The MOFs are then washed with DMF and then solvent exchanged with CHCl3. The MOFs were subjected to vacuum filtration with CHCl3 washes and air dried for 30 minutes. The MOFs were evacuated in a vacuum oven at 80 °C for solvent removal for characterization.

The general procedure for the lower benzaldehyde concentration of reductive amination of BDC-NH2 – KSU-1-RA. The MOF samples (~50mg) were transferred into an exchange thimble, that was placed in a 20 mL scintillation vial. The MOF samples were reacted in 0.51 mL of benzaldehyde (5.6×10^{-3} mol, 5M), 0.8 mL of 1M sodium cyanoborohydride (5.6×10^{-3} mol, 1M), and 4.49 mL of DMF in the presence of 3Å molecular sieves at room temperature and characterized every 2 days for a total of 6 days with continuous mixing on a TYZD-IIII Orbital Shaker. The MOFs are then washed with DMF and then solvent exchanged with $CHCl_3$. The MOFs were subjected to vacuum

filtration with CHCl3 washes and air dried for 30 minutes. The MOFs were evacuated in a vacuum oven at 80 °C for solvent removal for characterization.

The general procedure for the nucleophilic ring-opening of succinic anhydride – KSU-1-multi. Following the reductive amination post-synthetic step, KSU-1-RA (~30 mg) were transferred in an exchange thimble, that was placed in a 20 mL scintillation vial. The MOF samples were reacted with 0.4 mL of 1M succinic anhydride in anhydrous DMF (4.0 x 10-5 mol, 0.2M) and 1.6 mL of anhydrous DMF in the presence of 3Å molecular sieves at room temperature for 48 h with continuous mixing on a TYZD-IIII Orbital Shaker. The MOFs are then washed with DMF and then solvent exchanged with $CHCl_3$. The MOFs were subjected to vacuum filtration with CHCl3 washes and air dried for 30 minutes. The MOFs were evacuated in a vacuum oven at 80 °C for solvent removal for characterization.

Characterization

Powder X-ray diffraction (PXRD) patterns were recorded on a Bruker AXS D2 Phaser SSD160 diffractometer using nickel-filtered Cu Kα radiation (λ = 1.5418 Å) over a range of $5° < 2\theta < 40°$ in 0.1° steps with a 1-s counting time per step. Samples were collected from the bottom of the reaction vial as a thick suspension in DMF and spread on a Si-Einkristalle plate immediately before PXRD measurements. Given the high boiling point of DMF, the crystals never dry out during the PXRD measurement.

^{1}H NMR spectra were recorded on a Varian 400MHz NMR spectrometer (400 MHz for ^{1}H). NMR chemical shifts were reported in ppm against residual solvent resonance as the internal standard ($\delta(d_6DMSO) = 2.5$ ppm). Samples of MOF (~ 2 mg) were transferred into

an NMR tube and D_2SO_4 (0.01 mL, 98% w/w in D_2O) was added. The tubes were capped and sonicated until all the solid was dissolved (~ 1 min).

Chapter References

1. Morris, W.; Doonan, C. J.; Furukawa, H.; Banerjee, R.; Yaghi, O. M.; Crystals as Molecules: Postsynthesis Covalent Functionalization of Zeolitic Imidazolate Frameworks. Journal of American Chemical Society **2008**, *130*, 12626-12627.
2.Tanabe, K. K.; Wang, Z.; Cohen, S. M.; Systematic Functionalization of a Metal-Organic Framework via Postsynthetic Modification Approach. Journal of American Chemical Society, *130*, 8508-8517.
3. Dugan, E.; Wang, Z.; Okamura, M.; Medina, A.; Cohen, S. M.; Covalent modification of a metal-organic framework with isocyanates: probing substrate scope and reactivity. Chemical Communication **2008**, *0*, 3366-3368.
4. Savonnet, M.; Bazer-Bachi, D. Bats, N.; Perez-Pellitero, J.; Jeanneau, E.; Lecocq, V.; Pinel, C.; Farrusseng, D.; Generic Postfunctionalization Route from Amino-Derived Metal-Organic Frameworks. Journal of American Chemical Society **2010**, *132*, 4518-4519.
5. Doonan, C. J.; Morris, W.; Furukawa, H.; Yaghi, O. M.; Isorecticular Metalation of Metal-Organic Frameworks. Journal of American Chemical Society **2009**, *131*, 9492-9493.
6. Cordes, E. H.; Jencks, W. P.; On the Mechanism of Schiff Base Formation and Hydrolysis. Journal of American Chemical Society **1962**, *84*, 832-837.
7. Matsumoto, M.; Dasari, R. R.; Ji, W.; Feriante, C. H.; Parker, T. C.; Marder, S. R.; Dichtel, W. R.; Rapid, Low Temperature Formation of Imine-Linked Covalent Organic Frameworks Catalyze by Metal Triflates. Journal of American Chemical Society **2017**, *139*, 4992-5002.
8. Menche, D.; Bohm, S.; Li, J.; Rudolph, S.; Zander, W.; Synthesis of hindered tertiary amines by a mild reductive amination procedure. Tetrahedron Letters **2007**, 365-369.
9. Kalbasi, R. J.; Mazeaheri, O.; Facile one-pot tandem reductive amination of aldehydes from nitroarenes over a hierarchical ZSM zeolite containing palladium nanoparticles. New Journal of Chemistry **2016**, *40*, 9627.
10. Lee, O.; Law, K.; Yang, D.; Secondary Amine Formation from Reductive Amination of Carbonyl Compounds Promoted by Lewis Acid Using the ICl_3/Et_3SiH System. Organic Letters **2009**, *11*, 3302-3305.
11. Jagadeesh, R. V.; Murugesan, K.; Alshammari, A. S.; Neumann, H.; Pohl, M.; Radnik, J.; Beller, M.; MOF-derived cobalt nanoparticles catalyze a general synthesis of amines. Science **2017**, *358*, 326-332.
12. Wakchaure, V. N.; Zhou, J.; Hoffman, S.; List, B.; Catalytic asymmetric reductive amination of α-branched ketones. Angewante Chemie International Edition **2010**, *49*, 4612-4614.
13. Nakamura, Y.; Kon, K; Touchy, S.; Shimizu, K.; Ueda, W.; Selective synthesis of primary amines by reductive amination of ketones with ammonia over supported Pt catalysts.
14. Liang, G.; Wang, A.; Li, L.; Xu, G.; Yan, N.; Zhang, Y. T.; Production of primary amines by reductive amination of biomass-derived aldehydes/ketones. Angewante Chemie International Edition **2017**, *56*, 3050-3054.
15. Mao, F.; Sui, D.; Qi, Z.; Fan, H.; Chen, R.; Huang, J.; Heterogeneous cobalt catalysts for reductive amination with H_2: General synthesis of secondary and tertiary amines. Royal Chemical Society **2016**, *6*, 94068-94073.

16. Alinezhad, H.; Yavari, H.; Salehian, F.; Recent advances in reductive amination catalysis and its applications. Current Organic Chemistry **2015**, *19*, 1021-1049.
17. Gomez, S.; Peters, J. A.; Maschmeyer, T.; The reductive amination of aldehydes and ketones and the hydrogenation of nitriles: Mechanistic aspects and selectivity control. Advanced Synthesis & Catalysis **2002**, *344*, 1037-1057.
18. Keenan, L. L; Hamzah, H. A.; Mahon, M. F.; Warren, M. R.; Burrows. Secondary amine-functionalised metal-organic frameworks: direct syntheses *versus* tandem post-synthetic modifications. Crystal Engineering Communication **2016**, *18*, 5710.
19. Keenan, L. L.; Burrows, A. D.; Conversion of primary amines into secondary amines on a metal-organic framework using a tandem post-synthetic modification. Crystal Engineering Communication **2012**, *14*, 4112-4114.
20. Taylor-Pashow, K. M. L.; Rocca, J. D.; Xie, Z.; Tran, S.; Lin, W.; Postsynthetic Modifications of Iron-Carboxylate Nanoscale Metal-Organic Frameworks for Imaging and Drug Delivery. Journal of American Chemical Society **2009**, *131*, 14261-14263.
21. Saberi, D.; Akbari, J.; Mahdudi, S.; Heydari, A.; Reductive amination of aldehydes and ketones catalyzed by deep eutectic solvent using sodium borohydride as a reducing reagent. Journal of Molecular Liquids **2014**, *196*, 208-210.
22. Peng, L.; Calton, G. J.; Burnett, J. W.; Effect of borohydride reduction on antibodies. Applied Biochemistry and Biotechnology **1987**, *14*, 91-99.
23. Abdel-Magrid, A. F.; Carson, K. G.; Harris, B. D.; Maryanoff, C. A.; and Shah, R. D.; Reductive amination of Aldehydes and Ketones with Sodium Triacetoxyborohydride. Studies on Direct and Indirect Reductive Amination Procedures. Journal of Organic Chemistry **1996**, *61*, 3849-3862.
24. Fumagalli, C.; Succinc Acid and Succinic Anhydride. Kirk-Othmer Encyclopedia of Chemical Technology **2006**, *0*, 1-20.
25. Gadzikwa, T.; Farha, O. M.; Mulfort, K. M.; Hupp, J. T.; Nguyen, S. T.; A Zn-based, pillared paddlewheel MOF containing free carboxylic acids *via* covalent post-synthesis elaboration. Chemical Communications **2009**, *0*, 3720-3722.
26. Matsui, S.; Nitabaru, M; Yoshida, Y.; Mitani, M.; Fujita, T.; Olefin polymerization catalyst and process for olefin polymerization. 1008595. 2000.
27. Sisko, J.; Kassock, A. J.; Mellinger, M.; Filan, J. J.; Allen, A.; Olsen, M. A.; An Investigation of Imidazole and Oxazole Syntheses Using Aryl-Substituted TosMIC Reagents. Journal of Organic Chemistry **2000**, *65*, 1516-1524.
28. Cohen, S. M.; Modifying Mofs: new chemistry, new materials. Chemical Science **2010**, *1*, 32-36.
29. Tanabe, K. K.; Wang, Z.; Cohen, S. M.; Systematic Functionalization of a Metal-Organic Framework via a Postsynthetic Modification Approach. Journal of American Chemical Society **2008**, *130*, 8508-8517.
30. Britt, D.; Lee, C.; Uribe-Romo, F. J.; Furukawa, H.; Yaghi, O. M.; Ring-Opening Reactions within Porous Metal-Organic Frameworks. Inorganic Chemistry **2010**, *49*, 6387-6389.
31.Tanaka, K.; Kinoshita, M.; Kayahara, J.; Uebayashi, Y.; Nakaji, K.; Morawiak, M.; Urbanczyk-Lipkowska, Z.; Asymmetric ring-opening reaction of *meso*-epoxides with aromatic amines using homochiral metal-organic frameworks as recyclable heterogenous catalysts. RCS Advances **2018**, *8*, 28139-28146.

32. Chen, X.; Peng, Y.; Han, X.; Liu, Y.; Lin, X.; Cui, Y.; Sixteen isostructural phosphonate metal-organic frameworks with controlled Lewis acidity and chemical stability for asymmetric catalysis. Nature Communications **2017**, *8*, 1-9.
33. University of Wisconsin Department of Chemistry. Reactions of Amines: Reductive Amination (Borch Reaction). https://www.chem.wisc.edu/areas/clc/organic/345/FC/12_amines/05_reductive_amination.pdf (Accessed Sept. 10, 2018).

Chapter 4: Outlook

Introduction

Our idea to bifunctionalize KSU-1 with different PSM strategies serves as a proof of concept tool that can be used to independently functionalize KSU-1 uniformly. With our knowledge of KSU-1 and its structural characteristics, we have strategized to achieve orthogonal functionalization in KSU-1.

Strategy: Current Work and Future Direction

The synthetic strategy formulated to obtain a uniform orthogonally functionalizable KSU-1 involves a diazonium transfer of our amines to form azide functional groups. The resulting MOF, KSU-1-N_3, will have modifiable groups of orthogonal reactivity, -N_3 and -OH. The -N_3 can react with alkynes in a [3+2] cycloaddition, followed by a reaction with an anhydride for diester linkage formation by -OH (Scheme 13). We base our strategy off our prior knowledge of functional group selectivity and our foundational independently functionalizable reactions strategies.

As of now the diazonium transfer of KSU-1, our first PSM reaction, uses azidotrimethylsilane ($TMSN_3$) and t-butylnitrite (t-BuONO) in tetrahydrofuran (THF) to react with our amines to form azide functional groups.[1] This reaction shows promise and is currently under investigation to find optimal conditions that avoid the disassembly of KSU-1 during the reaction process. We want to do this reaction without damaging the structural integrity of KSU-1. The reagent that can cause the disassembly of the MOF is $TMSN_3$. $TMSN_3$ is known for its high reactivity and its formation of hydrazoic acid when exposed to a proton source.[2-3] Therefore, it is necessary to take extreme safety precaution when using $TMSN_3$.[4]

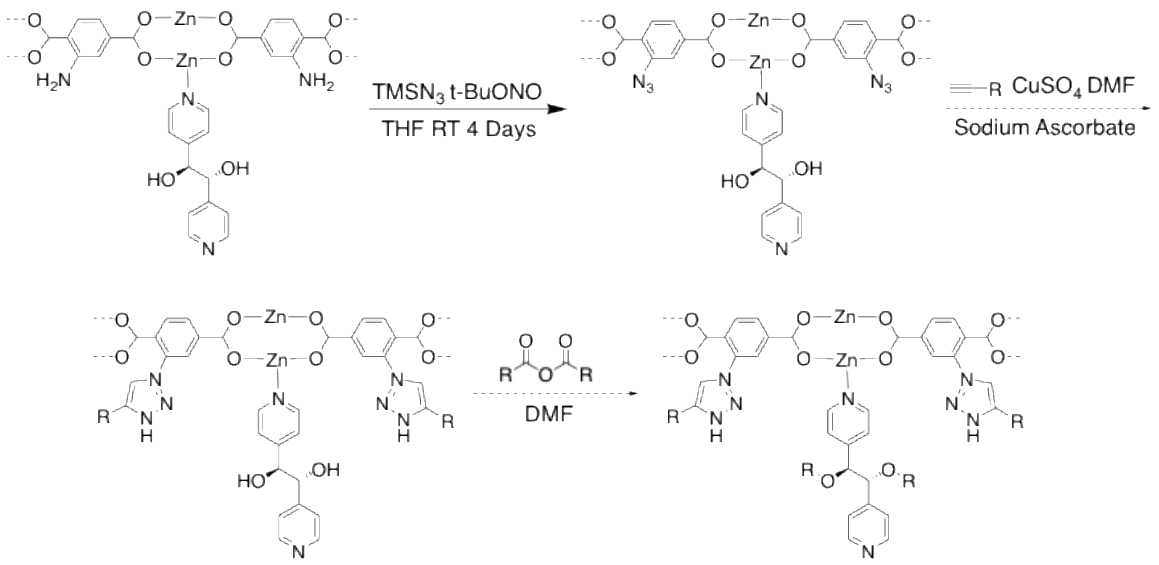

Scheme 13. A proposed PSM synthetic route for a fully orthogonal KSU-1.

Even though we had significant product loss throughout the reaction, we still had enough material for Fourier-transform infrared spectroscopy (FTIR) and ^{1}H NMR analysis. The FTIR shows the presence of an azide functional group with a peak at ~2100 cm^{-1} (Figure 13A). ^{1}H NMR (Figure 13B) suggests that the conversion of the amines to azides is complete based on the current conditions that destroyed the MOF. Our observed ^{1}H NMR for an azide conversion with BDC-NH_2 showed similarities to previously reported ^{1}H NMRs for the same reaction done by Savonnett *et al.*[1] This information was important for our data because in the ^{1}H NMR spectra we would expect to see two aromatic doublets and a singlet. Although this is not completely matched with the literature, we were relieved to see that an azide conversion from BDC-NH_2 has this behavior.

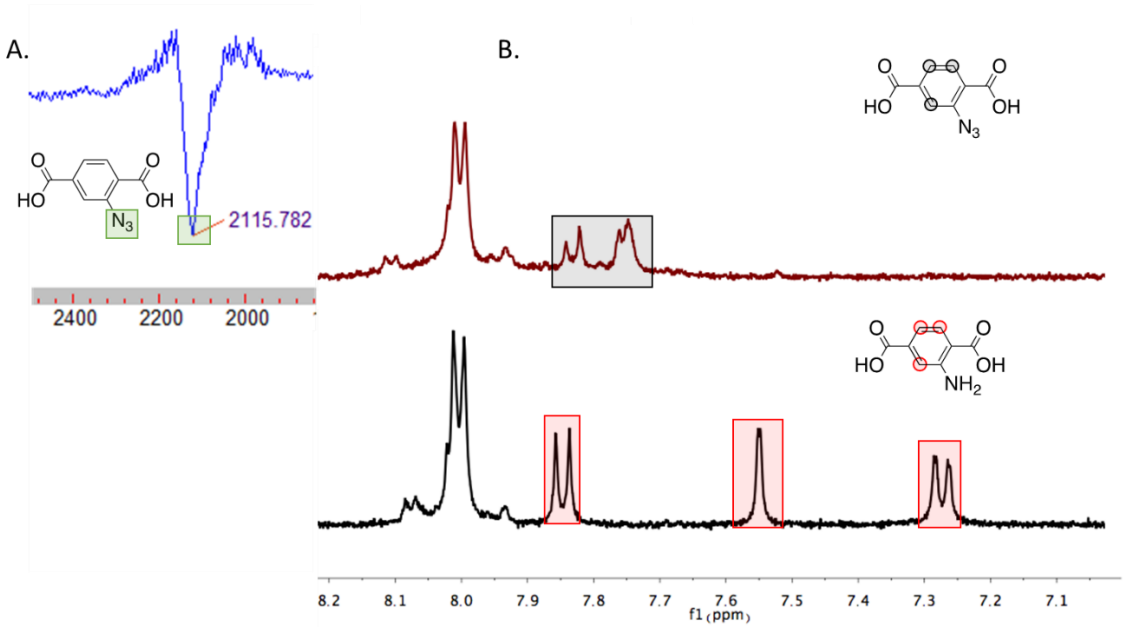

Figure 14. A) An FTIR vibrational frequency at 2116 cm-1 indicative of an azide functionality. B) 1H NMR of KSU-1-N3 and KSU-1.

Our next step in this process is to perform the [3+2] cycloaddition on the formed azide by using a reagent that has an alkyne group as a part of its chemical make-up. We are interested in this so called "click" chemistry due to the highly selective nature between azide and alkyne functional groups.[5] This selectivity is why "click" chemistry is used in an array of applications such a protein modification,[6] imaging,[7] catalysis,[8] etc. Click chemistry has been demonstrated in MOFs and through copper(I) catalyzed conditions.[14-16] Copper free conditions have also been used on the surfaces of MOFs.[17]

The copper(I) catalyzed reaction pathway is regularly used; but may not be preferential since it is difficult to maintain a Cu(I) oxidation state when exposed to certain conditions.[9] An alternative to using a copper catalyst is using copper free conditions that involve reagents that have ring structures with alkynes as part of the ring.[18] Alkynes have short bond lengths and perform 180° bond angles resulting in high ring strain. This leads to high reactivity to form 1,2,3 triazole groups involved in click chemistry. Since alkynes and

azides are highly selective towards each other, the alkyne will have no reactivity towards the alcohols of DPG showing our MOF has high selectivity in its design.

The alcohol functional groups will be reacted with an anhydride that is not highly reactive so that the MOF can be saved from some destruction as we have seen from time to time. When this last PSM modification is achieved, KSU-1 will be a uniform orthogonally functionalized metal-organic framework, the first of its kind.

Conclusion

The transformation of KSU-1 into its azide counterpart has seen some success, but due to the highly reactive nature of the $TMSN_3$ we are exploring optimal conditions with lower concentrations and a longer reaction time. KSU-1-N_3 will undergo Sharpless "click" chemistry with an alkyne functional group to make a 1,2,3-triazole and then a reaction with some anhydride with the alcohol functional groups DPG to obtain diesters. KSU-1 has a promising future in becoming fully orthogonal because of the blueprint of independent functionalization and a planned PSM synthetic strategy. Our mixed-ligand MOF, KSU-1, serves as the foundational infrastructure to become uniformly orthogonal based on specific post-synthetic modification reactions.

Experimental

The general procedure for the diazonium transfer of KSU-1 to KSU-1-N_3. This begins with the addition of KSU-1 (~30 mg) to an exchange thimble that is place into a 20 mL scintillation vial that already contains activated 3Å molecular sieves. 3mL of anhydrous THF is then placed into the vial. 0.66 mL (5.4×10^{-3} mols) of tert-butyl nitrite is added

slowly to the vial. The vial is then capped and allowed to react at room temperature on a TYZD-IIII Orbital Shaker for 1 h. After 1 h 0.6 mL (4.5×10^{-3} mols) trimethylsilyl azide is slowly added to the reaction mixture. The reaction resumes at room temperature on the shaker for 48 h.

Characterization

FTIR spectra was recorded on a Cary 630 FTIR. Samples of MOF (~1 mg) are transferred on to the crystal and compressed before spectra were observed.

^{1}H NMR spectra were recorded on a Varian 400MHz NMR spectrometer (400 MHz for ^{1}H). NMR chemical shifts were reported in ppm against residual solvent resonance as the internal standard ($\delta(d_6$DMSO) = 2.5 ppm). Samples of MOF (~ 2 mg) were transferred into an NMR tube and D_2SO_4 (0.01 mL, 98% w/w in D_2O) was added. The tubes were capped and sonicated until all the solid was dissolved (~ 1 min).

Chapter References

1. Savonnet, M.; Bazer-Bachi, D. Bats, N.; Perez-Pellitero, J.; Jeanneau, E.; Lecocq, V.; Pinel, C.; Farrusseng, D.; Generic Postfunctionalization Route from Amino-Derived Metal-Organic Frameworks. Journal of American Chemical Society **2010**, *132*, 4518-4519.
2. Birkofer, L.; Wegner, P.; Trimethylsilyl Azide. Organic Synthesis **1970**, *50*, 107.
3. Nishiyama, K.; Yamaguchi, T.; Selective Formation of Alkyl Azides Using Trimethylsilyl Azide and Carbonyl Compounds. Synthesis **1988**, *2*, 106-108.
4. Langerman, N.; Chemical Safety: Explosion hazard in synthesis of azidotrimethylsilane. Chemical and Engineering News **2014**, *92*, 1.
5. Kolb, H. C.; Finn, M. G.; Sharpless K. B.; Click Chemistry: Diverse Chemical Function from a Few Good Reactions. Angewandte Chemie **2001**, *40*, 2004-2021.
6. Finbloom, J. A.; Han, K.; Slack, C. C.; Furst, A. L. Francis, M. B.; Cucurbit[6]uril-Promoted Click Chemistry for Protein Modification. Journal of American Chemical Society **2017**, *139*, 9691-9697.
7. Zeng, Y.; Ren, J.; Shen, A.; Hu, J.; Splicing Nanoparticles-Based "Click" SERS Could Aid Multiplex Liquid Biopsy and Accurate Cellular Imaging. Journal of American Chemical Society **2018**, *140*, 10649-10652.
8. Darabedian, N.; Gao, J.; Chuh, K. N.; Woo, C. M.; Pratt, M. R.; The Metabolic Chemical Reporter 6-Azido-6-deoxy-glucose Further Reveals the Substrate Promiscuity of *O*-GlcNAc Transferase and Catalyzes the Discovery of Intracellular Protein Modification by *O*-Glucose. Journal of American Chemical Society **2018**, *140*, 7092-7100.
9. Himo, F.; Lovell, T.; Hilgraf, R.; Rostovtsev, V. V.; Noodleman, L.; Sharpless, K. B.; Folkin, V. V.; Copper(I)-Catalyzed Synthesis of Azoles. DFT Study Predicts Unprecedented Reactivity and Intermediates. Journal of American Chemical Society **2005**, *127*, 210-216.
10. Sarode, P. B.; Bahekar, S. P.; Chandak, H. S.; DABCO/AcOH Jointly Accelerated Copper(I)-Catalysed Cycloaddition of Azides on Water at Room Temperature.
11. Worrell, B. T.; Malik, J. A.; Fokin, V. V.; Direct Evidence of a Dinuclear Copper Intermediate in Cu(I)-Catalyzed Azide-Alkyne Cycloadditions. Science **2013**, *340*, 457-460.
12. Gadzikwa, T.; Lu, G.; Stern, C. L.; Wilson, S. R.; Wilson, S. R.; Hupp, J. T.; Nguyen, S. T.; Covalent surface modification of a metal-organic framework: selective surface engineering *via* Cu^{I}-catalyzed Huisgen cycloaddition. Chemical Communications **2008**, *0*, 5493-5495.
13. Cook, A. W.; Jones, Z. R.; Wu, G.; Scott, S. L.; Hayton, T. W.; An Organometallic Cu_{20} Nanocluster: Synthesis, Characterization, Immobilization on Silica, and "Click" Chemistry. Journal of American Chemical Society **2018**, *140*, 394-400.
14. Tuci, G.; Rossin, A.; Xu, X.; Ranocchiari, M.; van Bokhoven, J. A.; Luconi, L.; Manet, I.; Melucci, M.; Giambastiani, G.; "Click" on MOFs: A Versatile Tool for the Multimodal Derivatization of N_3-Decorated Metal Organic Frameworks. Chemistry of Materials **2013**, *25*, 2297-2308.
15. Lu, B.; Yang, J.; Che, G.; Pei, W.; Ma, J.; Highly Stable Copper(I)-Based Metal-Organic Framework Assembled with Resorcin[4]arene and Polyoxometalate for Efficient

Heterogeneous Catalysis of Azide-Alkyne “Click” Reaction. ACS Applied Materials & Interfaces **2018**, *10*, 2628-2636.
16. Gadzikwa, T.; Farha, O. K.; Malliakas, C. D.; Kanatzidis, M. G.; Hupp, J. T.; Nguyen, S. T.; Selective Bifunctional Modification of a Non-catenated Metal-Organic Framework Material via “Click” Chemistry. Journal of American Chemical Society **2009**, *131*, 13613-13615.
17. Morris, W.; Briley, W. E.; Auyeung, E.; Cabezas M. D.; Mirkin, C. A.; Nucleid Acid-Metal-Organic Framework (MOF) Nanoparticle Conjugates. Journal of American Chemical Society **2014**, *136*, 7261-7264.
18. Yoon, H. I.; Yee, J. Y.; Na, J. H.; Lee, S.; Lee, H.; Kang, S.; Chang, H.; Rye, J.; Lee, S.; Kwon, I. C.; Cho, Y. W.; Kim, K.; Bioorthogonal Copper Free Click Chemistry for Labeling and Tracking of Chondrocytes *In Vivo*. Bioconjugate Chemistry **2016**, *27*, 927-936.
19. Favre, C.; Friscourt, F.; Fluorogenic Sydnone-Modified Coumarins Switched-On by Copper-Free Click Chemistry. Organic Letters **2018**, *20*, 4213-4217.
20. Fruh, S. M.; Steuerwald, D.; Simon, U.; Vogel, V.; Covalent Cargo Loading to Molecular Shuttles via Copper-free “Click Chemistry”. Biomacromolecules **2012**, *13*, 3908-3911.
21. Chakrabarty, R.; Stang, P.; Post-assembly Functionalization of Organoplatinum(II) Metallacycles via Copper-free Click Chemistry. Journal of American Chemical Society **2012**, *134*, 14738-14741.
22. Han, Y.; Yuan, L.; Li, G.; Huang, L.; Qin, T.; Chu, F.; Tang, C.; Renewable polymers from lignin via copper-free thermal click chemistry. Polymer **2016**, *83*, 92-100.
23. Ghandiyar, S.; Hamzehloueian, M.; Hosseinzaldeh, R.; Mechanism study on the copper-free click reaction of a coumarin-conjugated cyclooctyne. Structural Chemistry **2017**, *28*, 1969-1979.